Universitat de Vic
Escola Politècnica Superior

Institut de Ciència i Tecnologia Ambientals · UAB

**Final degree project**

# *Impacts of ocean acidification and warming on planktic foraminifera in the Catalan Sea (Western Mediterranean) during the last centuries.*

Ariadna Baró Planella

**Degree in Environmental Sciences**

Tutors: Patrizia Ziveri and Graham Mortyn

Guarantor: Josep Ayats i Bansells

Vic, September 2017

**ABSTRACT OF THE FINAL DEGREE PROJECT**

**DEGREE IN ENVIRONMENTAL SCIENCES**

**Title:** *Impacts of ocean acidification and warming on planktic foraminifera in the Catalan Sea (Western Mediterranean) during the last centuries.*

**Key words:** Mediterranean Sea, ocean acidification, ocean warming, foraminifera.

**Author:** Ariadna Baró Planella

**Tutors:** Dra. Patrizia Ziveri (ICTA), Graham Mortyn (ICTA) and Josep Ayats Bansells (UVic)

**Data:** September 5 de 2017

This final degree project is part of the practice's realized at research institute ICTA-UAB (Institut de Ciència i Tecnologia Ambientals), which consisted in the analysis of an oceanic sedimentological register. Core 1 was obtained in May 2013, adjacent to Barcelona's coast, latitude 41.1121 N and longitude 2.382 E, at 1156 m water depth at the end of the MedSeA Cruise, in order to collect further data for the project. Once collected, the core was transported to ICTA where during 2016 the upper half part of Core 1 was analyzed by Griselda Anglada as a part of her Master's Thesis.

Following the same procedures, planktic foraminifera of the bottom part of core 1 were extracted from the remaining lower samples and separated by fractions, whereby the most common foraminiferal species in the size fraction between 250 to 315 µm were picked from each half centimetre of the sediment core, determining its absolute and relative abundance. Then specimens of the five most abundant species were selected, weighed and image analyzed to determinate its Size-Normalized weight (SNW).

The main aim is to reconstruct the dynamics of planktonic calcifiers in the Catalan Sea (Western Mediterranean) during the last ˜400 years, through the characterization of the species absolute abundance, relative abundance and SNW. This study will contribute to the understanding of the natural variability and the recent impacts of elevated atmospheric CO2, determining ocean warming and acidification effects in the region. For this reason the results obtained by Griselda were coupled with those of the bottom part in order to get core 1 completed and later analyze the obtained results.

The sediments have been dated with the aim of relating the obtained results with the following reconstructed physical parameters: atmospheric $CO_2$ concentration, Sea Surface Temperature (SST), North Atlantic Oscillation and Total Solar Irradiation. Through statistical correlation by Pearson's coefficient, I determined the possible effects on the dynamics of the foraminiferal analyzed species.

The results indicate changes in ecological conditions all over the studied period, but especially from approximately year CE 1840 until today due to the considerable increase of atmospheric $CO_2$ that penetrates to the superficial sea waters and has modified the water column conditions and also altered species absolute abundance, relative abundance and SNW.

The statistical results of Pearson's correlation coefficient show that an abundance decrease and a calcification increase has happened during the studied period. Acidification, through the increase of $CO_2$, is the principal cause of the reduction in foraminiferal abundance, while the increase on solar irradiation is the main cause of calcification increase. Warming is harmful for foraminifera due to SST increase reducing both abundance and calcification.

# Content

# 1. Introduction

During all Earth's history the ocean has been playing a key role in global climate dynamics and biogeochemical cycles due to its large extension covering approximately 71 % of the total planet's surface. Oceans are an important sink of CO2 keeping in chemical equilibrium with the atmosphere, exchanging large amounts of carbon dioxide ($CO_2$), and absorbing about 1/3 of the total released atmospheric CO2 since the Industrial Revolution (REFS). This global carbon cycle is one of the most important biogeochemical cycles, but recently it has been disrupted by anthropogenic activities.

The pre-industrial influx from the ocean to the atmosphere was 70.6 Gt C $yr^{-1}$, while the flux in the opposite direction was 70 Gt C $yr^{-1}$ (Alley et al., 2007). Since the Industrial Revolution, a significant increase in atmospheric CO2 concentration of anthropogenic origin, that is now above 400 ppm (US Department of Commerce, NOAA, 2017), is the main reason that the anthropogenic flux has exceeded the natural flux.

The greenhouse effect acceleration and sea level rise are the main consequences of greenhouse gas release of into the atmosphere, such as CO2, which currently is 30% higher than in the past 200 years (Bauska et al., 2015; US Department of Commerce, NOAA, 2017). Ocean acidification is another but lesser known consequence.

The main aims of this final degree project are the following:

**.** Reconstruct the dynamics of planktonic calcifiers in the Catalan Sea (Western Mediterranean) during the last ˜400 years, through the characterization of the species absolute abundance, relative abundance and SNW.

**.** Contribute to the understanding of the natural variability and the recent impacts of elevated atmospheric CO2, determining ocean warming and acidification effects in the region.

## 1.1. Ocean Acidification

Ocean acidification refers to a reduction in the pH of the ocean over an extended period, typically decades or longer, caused primarily by the uptake of $CO_2$ from the atmosphere, but it can be caused by other chemical additions or substances from the ocean. In the case of this final degree project we will talk about anthropogenic ocean acidification that refers to the component of pH reduction caused by human activity.

The global carbon cycle with its ocean-atmosphere exchange, disrupted by anthropogenic activities, is the cause of oceanic acidification. This process is carried out as described below:

The cycle is based on TIC **(1)** or Total Inorganic Carbon, which is the total sum of the dissolved carbonate species in seawater. Once atmospheric $CO_2$ is dissolved in seawater **(2)** and, because of its instability, reacts with water forming carbonic acid **(3)**. This, depending on temperature and salinity, dissociates into bicarbonate ions **(4)**, which also dissociate to produce carbonate ions **(5)**. Acid (H+) is released by these processes and, consequently, seawater pH and carbonate ion concentration both decrease (Zeebe, 2012).

The concentration of protons ($[H^+]$), which is proportional to the ratio $[HCO_3^-]/ [CO_3^{2-}]$, increases and pH decreases. The surface-ocean pH expressed by the logarithm of H+ concentration **(6)**, has decreased from approximately 8.2 to 8.1 between pre-industrial time and the 1990s. A decline of 0.1 pH units seems insignificant but means an increasing of a 30% of $CO_2$ concentration in seawater. Meanwhile in the last 20 million years pH has probably been constant, not below 8.2 (Schellnhuber, Cramer, Nakicenovic, Wigley, & Yohe, 2006) and according to J.-P Gattuso & Lavigne, 2009 following this tendency the pH may reach 7.8 in 2100 entailing serious consequences.

**1.** $TIC = [CO_2] + [HCO_3^-] + [CO_3^{2-}]$ **2.** $[CO_2\ (g)] = [CO_2\ (aq)]$

**3.** $CO_2\ (aq) + H_2O \leftrightarrow H_2CO_3$ **4.** $H_2CO^3 \leftrightarrow HCO_3^- + H^+$

**5.** $HCO_3^- \leftrightarrow CO_3^{2-} + H^+$ **6.** $pH= \log[H^+]$

### 1.1.1. Effects of ocean acidification

As a consequence of ocean acidification all biological and biogeochemical processes are potentially directly and indirectly affected. Disturbances in the acid-base status of organisms may be created while pH plays a key role in many physiological processes, such as ion transport, enzyme activity and protein function.

In the case of calcifying organisms and the global calcium carbonate cycle, ocean acidification will be an important outcome because of the increasing concentration of bicarbonate ions and dissolved inorganic carbon ($C_T$), lowers the pH, the concentration of carbonate ions and the saturation state of the three major carbonate minerals present in shells and skeletons **(7)**. Calcification and precipitation decrease with increased acidification of the ocean, which may lead to a decrease in the calcification rate **(8)**. In contrast, the reverse reaction of dissolution of calcium carbonate is favoured by the decrease in the $CaCO_3$ saturation state generated by ocean acidification **(9)**.

**7.** $CO_2 + H_2O + CO_3^{2-} \rightarrow 2\ HCO_3^-$

**8.** $Ca^{+2} + 2\ HCO_3^- \rightarrow CaCO_3 + CO_2 + H_2O$

**9.** $Ca^{+2} + CO_3^{2-} \rightarrow CaCO_3$

On the other hand weathering is the source of ocean alkalinity and regulates ocean acidification. For each mole of $CO_2$ absorbed during $CaCO_3$ weathering, one mole of $CO_2$ is released during $CaCO_3$ precipitation **(10)**. In addition, silicate mineral weathering **(11)** removes $CO_2$ from the atmosphere and buries it as $CaCO_3$ in sediments. Under high $CO_2$, silicate weathering and carbonate formation are enhanced and this cycle becomes responsible for carbon sequestration, but this is balanced over a longer time scale (Zeebe, 2012).

**10.** $CaCO_3 + CO_2 + H_2O \rightarrow Ca^{+2} + 2\ HCO_3^-$

**11.** $CaSiO_3 + CO_2 + H_2O \rightarrow CaCO_3 + SiO_2 + H_2O$

By this way, the expression ‘ocean acidification’ refers to the decrease in pH but does not imply that the pH of surface-ocean waters will become acidic. The whole process could equally be referred to as ‘carbonation’ as it increases the concentration of dissolved inorganic carbon (Jean-Pierre. Gattuso & Hansson, 2011). The increase in surface-ocean dissolved $CO_2$ is proportional to that in the atmosphere (upon equilibration after about 1 year) but the increase in $C_T$ is not, as a result of the buffer capacity of seawater. The relative change of dissolved $CO_2$ to the relative change of $C_T$ in the seawater equilibrium with atmospheric $CO_2$ is described by the Revelle factor

according to which a doubling in atmospheric $CO_2$ only leads to an increase in $C_T$ of about 10% (Zeebe & Wolf-Gladrow, n.d.). (Egleston, Sabine, & Morel, 2010) have shown that the adsorption of $CO_2$ from the atmosphere will be less efficient and that $[CO_2]$, $[H^+]$, and saturation states and will be more sensitive to environmental changes (Jean-Pierre. Gattuso & Hansson, 2011).

Also changes in photosynthesis influence the thermodynamics and kinetics of metals and some nutrients in seawater, affecting the availability and toxicity of metals to marine organisms. A tight link may exist between processes such as photosynthesis and calcification. Photosynthesis by ocean acidification could benefit calcification by mitigating the limited supply of carbonate ions. Conversely, if calcification stimulates photosynthesis, a decrease in calcification generated by ocean acidification could have a negative effect on photosynthesis. Such cascading, indirect effects could occur at both the organism and community levels.

The impacts of acidification can be much more substantial in some areas of the coastal ocean and in marginal seas like the Mediterranean Sea, at the order of 10-50% or more. Future decrease of seawater pH can result either from the passive uptake of atmospheric $CO_2$ as described above or from purposeful dumping of liquid $CO_2$ into deep ocean (for $CO_2$ disposal) (Jean-Pierre. Gattuso & Hansson, 2011).

## 1.2. Ocean Warming

Plankton plays a key role in the oceans. It forms the basis of the marine food web and is quantitatively important for reducing the greenhouse effect on earth. Phytoplankton growth depends on light and on nutrients such as nitrogen and phosphorus. These nutrients are supplied from deeper ocean layers, and are slowly mixed upwards.

Warmer temperatures lead to faster metabolic rates, which will likely increase primary and $CaCO_3$ production into the photic zone. However, the increase of warm surface layers reduce mixing of the ocean waters. A larger temperature difference between two water layers implies less mixing of chemicals between these water layers, producing a phenomenon called stratification. This may cause shifts in plankton species disadvantaging foraminiferal composition and favouring other organisms those increase $CaCO_3$ production and reducing the $CO_2$ uptake.

## 1.3. The Mediterranean Sea

Mediterranean Sea, lying between latitudes 30° and 46° N and longitudes 5°50′ W and 36° E **(Figure 1)**, is the world's largest inland sea with a surface of 2.499.350km$^2$ that represents approximately 0.8% of the world's ocean surface area (Hassoun et al., 2015) and has an average depth of 1.500 m. The Mediterranean Sea is almost land-locked with the exception of the Strait of Gibraltar, which links the Mediterranean Sea with the Atlantic Ocean becoming its major source of water circulation removal. Moreover the Mediterranean Sea is also connected with the Black Sea by the Sea of Marmara and with the Red Sea by the human made Suez Canal. In total the sea is surrounded by the continents of Europe, Asia, and Africa and borders more than 21 different nations. The Mediterranean has more than 3,000 islands and archipelagos.

The Strait of Sicily between Sicily and Cape Bon, Tunisia, divides the Mediterranean into two main basins **(Figure 1)**. The Western Mediterranean that contains the sub-basins of the Alboran Sea, Balearic Sea, Ligurian Sea and Tyrrhenian Sea; and the Eastern Mediterranean that contains the sub-basins of the Adriatic Sea, Ionian Sea, Aegean Sea and Levantine Sea. The Western Basin extends from the Cape of Trafalgar in Spain and the Cape of Spartel in Africa in the west, to Tunisia's Cape Bon in the east. The Eastern Basin stretches from the eastern boundary of the Western Basin to the coasts of Syria and Palestine.

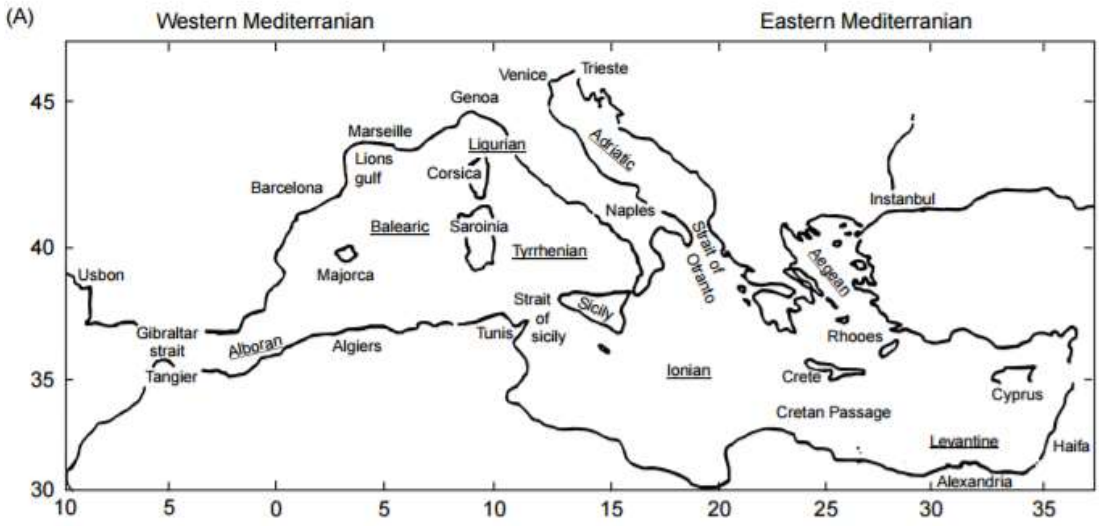


**Figure 1.** The Mediterranean Sea geography and nomenclature of the major sub-basins and straits. Source: Thorpe, 2009

### 1.3.1. Ocean Circulation

(from Rohling, Marino, & Grant, 2015)

The Mediterranean circulation is driven by thermohaline forcing, whereby temperature and salinity increases eastward due to evaporation. Relatively fresh and cold waters from the Atlantic, Atlantic Water (AW), enters the Mediterranean Sea through the Strait of Gibraltar and mixes with warmer and saltier upwelled Mediterranean Intermediate Water (MIW), creating Modified Atlantic Waters (MAW) with higher salinities. This water mass flows eastward and going across the Strait of Sicily to the western Mediterranean basin by the transport of Atlantic Water, the major forcing of exchange, rather than the density gradient between the western and the eastern Mediterranean. In the Levantine Sea denser and saltier waters are formed close to the continent due to cold winter air masses towards the sea, which enhance evaporation and favour water column vertical convection. In this way, the Levantine Intermediate Water (LIW) is formed. Then, it flows westward deeply into the Strait of Sicily, between 150 and 600 m water depth, and is separated from shallow MAW in a transitional water column by the halocline. While LIW flows westward and approaches the Strait of Sicily, some of this water mass is re-circulated back into the eastern basin, meanwhile the rest goes to the Western Mediterranean basin. Along its path to the Strait of Gibraltar, LIW reduces its temperature and salinity by an admixture with low salinity waters (TDW). Also involved and below LIW, at about 1km depth, there are well-oxygenated deep and bottom waters in each western and eastern Mediterranean basins called Eastern and Western Mediterranean Deep Water. Eastern Mediterranean Deep Water (EMDW) is formed in the Adriatic and Aegean Seas, and the Western Mediterranean Deep Water (WMDW) in the Gulf of Lions.

The Mediterranean Sea has a vigorous thermohaline circulation that transforms relatively warm (temperature of 15–16°C) and fresh (salinity of 36.1–36.2 PSU) Atlantic surface waters that enter into the basin through the Strait of Gibraltar to cooler (temperature of ~13°C) and saltier waters (salinity of ~38.5 PSU) (Wüst, 1961) that return to the North Atlantic at depth through the strait, having experienced both net evaporation and net cooling (Garrett, 1994). The resulting density difference between the Mediterranean and the Atlantic Ocean forces the Mediterranean Outflow and becomes responsible for its generally oligotrophic and relatively well oxygenated conditions (Hassoun et al., 2015).

In detail, 4 or 5 water masses may contribute to the total exchange through the Strait of Gibraltar (Millot, 2009). All Mediterranean water masses are closely related, so that significant modification to one will also affects the others. The freshwater flux through the Mediterranean Sea surface is a key control on the exchange between the Atlantic and the Mediterranean (Béranger, Mortier, & Crépon, 2005).

### 1.3.2. CO2 dynamics

(from Hassoun et al., 2015)

The Mediterranean Sea is very special in terms of $CO_2$ dynamics, global carbon cycle and anthropogenic $CO_2$ drawdown and storage (Hassoun et al., 2015). Because of its negative freshwater balance due to evaporation, little precipitation and river discharge, the Mediterranean Sea's warm and high alkalinity waters are prone to absorb $CO_2$ from the atmosphere and be transported to the interior by the active overturning circulation (Álvarez, 2011). The anthropogenic $CO_2$ inventory for the Mediterranean has been estimated to be 1.7 PgC (Sabine & Tanhua, 2010), thus indicating that this marginal sea has higher $C_{ANT}$ (Anthropogenic carbon) concentrations than the global average and much higher than those recorded in oceanic areas.

According to the article the most invaded waters by $C_{ANT}$ are the intermediate (300–500 m) and deep (>500 m) layers of the Alboran, Liguro and Algero-Provencal Sub-basins in the Western basin, and the Adriatic Sub-basin in the Eastern basin. Whereas the areas containing the lowest $C_{ANT}$ concentration are the deep layers of the Eastern basin, especially those of the Ionian Sub-basin and those of the northern Tyrrhenian Sub-basin in the Western basin where the concomitant low $O_2$ concentrations indicate that the prevailing waters are very old. In general, the Eastern basin accumulates less $C_{ANT}$ than the Western basin because of two facts: its deep water renewal time that has been estimated to be 20-40 years in the western basin (Stratford, Williams, & Drakopoulos, 1998) and about 100 years in the eastern basin (Stratford & Williams, 1997) and the lower solubility and penetration of atmospheric $CO_2$ because of its high surface temperature and salinity.

The accumulation of $C_{ANT}$ resulted in a significant reduction of pH compared to the preindustrial era, as mentioned by Touratier & Goyet, 2009. The pH increases Eastward, being more acid the waters of the Western basin rather than those of the Eastern basin.

Their results indicate that both Mediterranean Sea basins are supersaturated with calcite and aragonite, respectively; the Western basin is characterized by carbonate ions concentrations and saturations degrees lower than those in the Eastern basin. This shows that, at a large time scale, the pH decrease can influence the dissolution of carbonate ions and then the biological activity of several marine organisms, especially the calcifying ones.

### 1.3.3. Catalan-Balearic Sea

The Balearic Sea, Catalan Sea or Iberian Sea is a semi-enclosed basin from the northwestern Mediterranean Sea bounded by the Iberian Peninsula in the west and northwest, and in the southeast by the archipelago of the Balearic Islands (Mallorca, Menorca, Cabrera, Ibiza and Formentera). At its southeastern edge the Balearic Sea merges with the Alboran Sea; in the northeast it is open to the Gulf of Lions, it is separated from the Tyrrhenian Sea to the east by Sardinia and Corsica and abuts the sea to the west, while in the southeast it is connected to the Algerian Basin by means of three gaps in the islands (Ibiza, Mallorca and Minorca Channels). The bathymetry is dominated by the Balearic Abyssal Plain, which covers over 77.6997 square kilometers, covering the majority of the basin floor at depths ranging from 2700 to 2800 meters. The Ebro is the most important river that flows into this small sea.

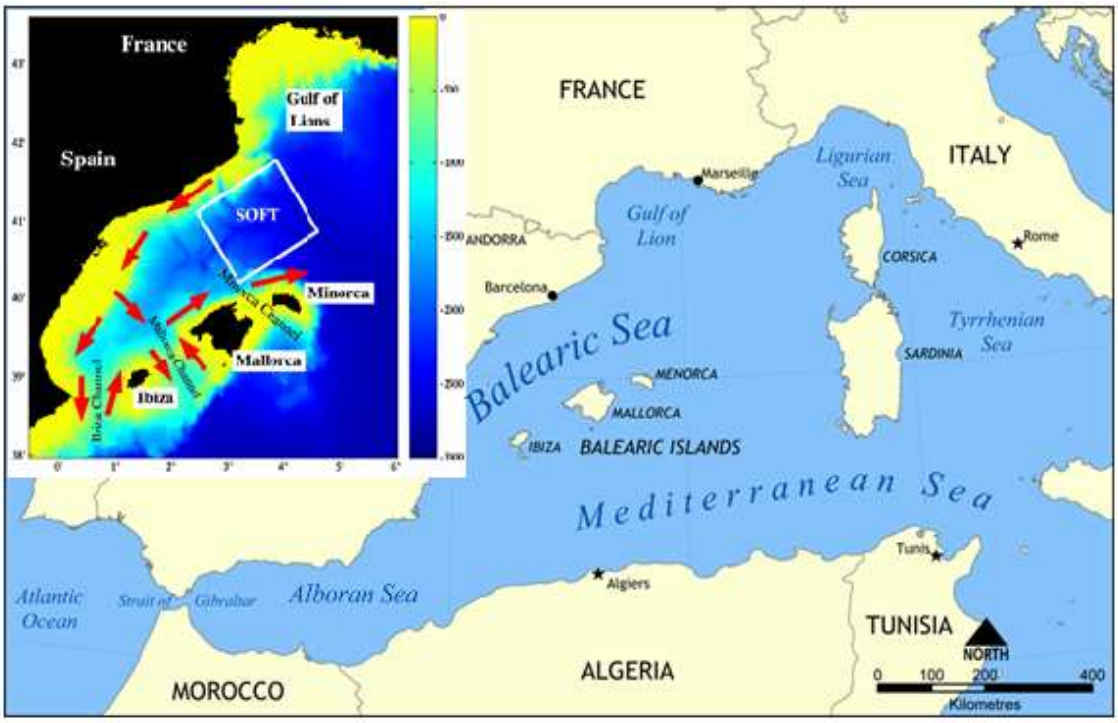


**Figure 2.** Location map of western Mediterranean basin focused on Balearic Sea (NormanEinstein, May 26, 2006) and its water circulation (Onken et al., 2008).

From the surface to 150 meters depth in the Balearic Sea, Modified Atlantic Water (MAW) is dominant. Those waters originating from the Strait of Gibraltar invade the basin from the south through the Ibiza Channel, then older MAW coming from the Liguro-Provençal-Catalan Current in the north go along the Iberian shelf slope and continues south along the slope. This current is divided and one partly keeps on heading farther south leaving the Balearic Sea through the Ibiza and Mallorca Channels and the other part makes a cyclonic turn at about the latitude of the

Mallorca Channel and joins there the MAW flow from the south forming the Balearic Current, which is closely attached to the northeastern slopes of Mallorca and Minorca, and leaves the basin heading northeast. This basin-scale circulation pattern from the Liguro-Provençal-Catalan and Balearic Currents is accompanied by the Catalan and the Balearic Front. Below the MAW, to approximately 700 meters depth, the LIW current is coming from the north and joins the large-scale cyclonic circulation similar to the MAW. Finally, the Western Mediterranean Deep Water originating from deep convection events in the Gulf of Lions fills the deep basin (Onken et al., 2008).

## 1.4. Foraminifera

(from Schiebel & Hemleben, 2017)

Planktic foraminifers are unicellular heterotrophic marine protozoa with calcareous shells and chambered tests. Its internal cytoplasm contains organelles that allow them to float. They can be omnivores or carnivores and consume phytoplankton, mainly diatoms and dinoflagellates. Their first appearance was approximately 170 million years ago, in the mid-Jurassic, and they were populating the whole oceans in global marine abundance since the Lower Cretaceous, 110 Million years ago. The size of planktonic foraminifera is less than one mm and at naked eyes seems like a grain of sand. Planktic foraminifera are the main producers of marine calcareous particles deposited in the ocean.

Due to the high preservation potential of their calcareous shell, planktic foraminifers provide information on the past environment and climate, providing a good archive in paleoceanography studies. Physical conditions and chemical composition of ambient seawater are reconstructed from the presence or absence of foraminifer species, as well as through the chemical composition of their test calcite, including crystallinity of the test wall, and changes in stable isotope and element ratios.

Most modern species live in the surface layer of the thermocline of the open ocean, and in deeply marginal seas like the Mediterranean. It is possible to find species from the surface of the ocean to the abyssal zone at more than 400 m depth. The presence and absence of planktonic foraminifera species at regional scale is related to the quality and quantity of food, the physical and chemical properties of the environmental sea water and shows a global latitudinal pattern on a planetary scale. The abundance of species varies according to the seasons, as well as on an

inter-annual scale, and on longer time scales depending on the environmental conditions and affected by climate change.

According to DNA sequencing based on a maximum likelihood reconstruction from SSU rDNA, from WEINER, AURAHS, KURASAWA, KITAZATO, & KUCERA, 2012 modified after by Aurahs et al., 2009, taxonomic and phylogenetic relations can be established for the different planktic foraminifer's morphospecies. Modern planktic foraminifers are divided by four major groups; macroperforate spinose, macroperforate non-spinose, microperforate spinose, and hastigerinidae distinguished by their test architecture. **(Figure 3)**

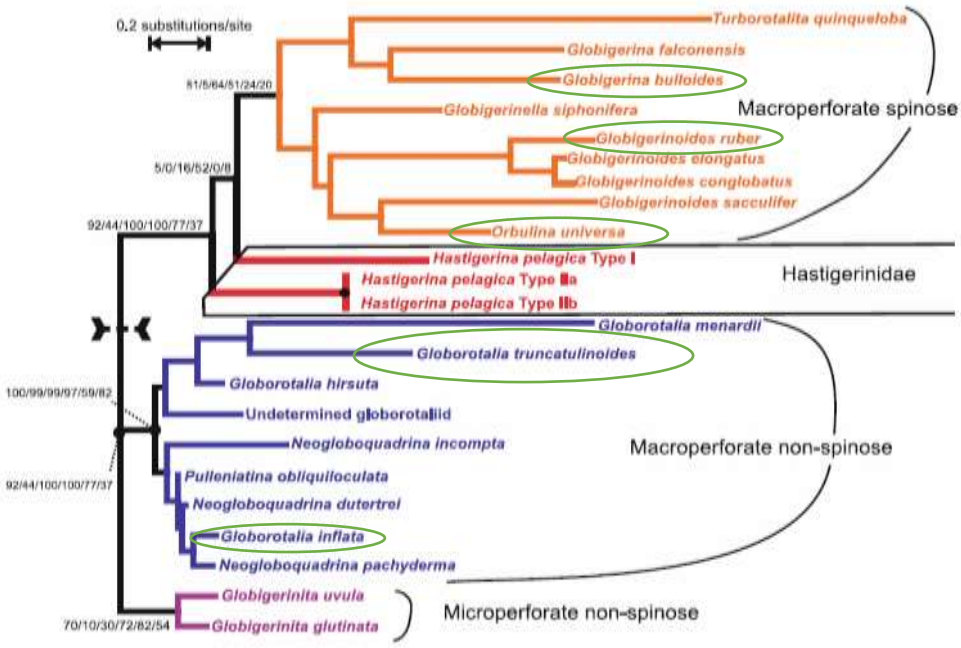


**Figure 3.** Phylogenetic relationships of the four major groups of modern planktic foraminifers. Source: From the book Planktic Foraminifers on the common era by Schiebel & Hemleben, 2017**.**

Below, the most abundant species of planktic foraminifera found in core 1 of the Catalan Sea (Mediterranean Sea), highlighted in the previous picture **(Figure 3),** are going to be explained in more detail, ordered from the shallowest to the deepest species.

### 1.4.1. *Globigerinoides ruber*

(G. ruber pink, G. ruber sensu sricto and G. ruber sensu lato)

This is classified as macroperforate spinose due to its pore-size, bigger than 1 μm and spines. Its characteristic features are: the test has 3 globular chambers per whorl, their last three chambers adjoin the umbilical primary aperture and two smaller secondary apertures are formed on the spiral side.

*Globigerinoides ruber* is the most abundant species between tropical to subtropical waters of the global ocean. They are the most adaptable of *Globigerinoides* species to ecological conditions because they accept slightly higher ratios of phytoplankton prey than the other species and have symbiosis with dinoflagellates. Controlled laboratory experiments have determined that *Globigerinoides ruber* can live in a range of temperature and salinity of 14 to 31 °C and 22–49 PSU respectively; for this reason it is said by Rohling et al., 2004 that *Globigerinoides ruber* is the most tolerant species to low Sea Surface Salinity (SSS), caused by continental fresh water runoff into the ocean. As a consequence they live in the upper part of the sea.

*Globigerinoides ruber* presents two phenotypes, a white (*G. ruber* white), and a pink variety (*G. ruber* pink) stained by pigments which at the present date are still unknown. *G. ruber* pink is bigger than the white variety (grows 50 μm more). The white variety can be found in all actual ocean basins. Conversely the pink variety today only exists in the Atlantic Ocean and Mediterranean Sea, where in the other seas it became extinct during the Pleistocene epoch due to its restricted specific ecological demands. *G. ruber* pink is considered a 'summer species' because it prefers warmer habitats than *G. ruber* white (Bé, 1967). The wide acceptance of different food sources and abundance from upwelling (eutrophic) regions to subtropical (oligotrophic) gyres (Rohling et al., 2004) and a year-round occurrence with a fortnightly frequency reproduction, allow *G. ruber* white to be in all the oceans with high abundance and extended distribution.

According to Aurahs, Treis, Darling, & Kucera, 2011 G. ruber plexus comprises six genetically defined types (Ia, Ib, IIa, IIb, pink, and conglobatus) **(Fig 4b)**, as well as several subtypes that can be seen in **Fig 4a**:

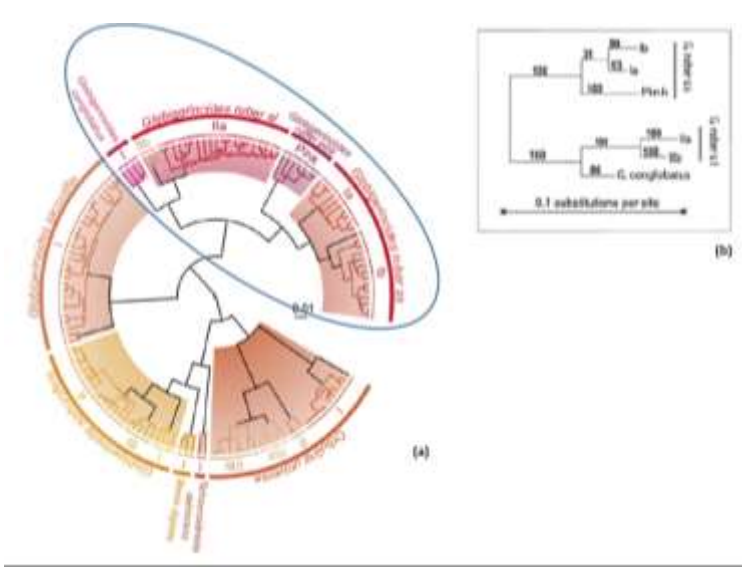

**Figure 4. (a)** Ultrametric tree based on SSU rDNA of spinose species including *G. ruber* and related species, with significant GMYC delimitations. Colored branches correspond to GMYC clusters. The outer circle corresponds to the names of the morphospecies. Plausible biological species are given on the inner arc. from André et al., 2014 **(b)** Graphical distances between six genotypes and their subtypes of the *G. ruber* plexus based on SSU rDNA data from Aurahs et al., 2011. Source: (Schiebel & Hemleben, 2017)

Most of these types are restricted to certain ocean basins. The types Ia, Ib, and IIa can be found globally, while type IIb occurs in the Mediterranean Sea and the pink type in the Atlantic Ocean and the Mediterranean Sea.

In the Mediterranean Sea there are two white ruber predominant morphotypes, *G. ruber* sensu stricto and *G. ruber* sensu lato; *G. ruber* sensu stricto (Ia) has a symmetrical test with spherical chambers formed and a high arched primary aperture and *G. ruber* sensu lato (IIa) includes compact tests with non-spherical, slightly compressed chambers formed by the adult specimen, which results in a relatively small primary aperture and presents kummerform. In addition there is a specific type of *G. ruber* sensu lato in the Mediterranean (IIb) that has a third elongate with a high-trochospiral test.

Plankton tow and sediment trap studies show that *G. ruber* sensu stricto generally inhabits the upper 30 m of the water column, while *G. ruber* sensu lato calcifies at cooler temperatures and/or deeper depths up to 50 m (Brown, Flower, & Williams, 2012).

**Figure 5.** Picture of the tree different *Globigerinoides ruber* types most common found on the Mediterranean Sea, from left to right: *G. ruber* pink, *G. ruber* sensu stricto and *G. ruber* sensu lato.

### 1.4.2. *Globigerina bulloides*

This is classified as macroperforate spinose due to most of its pore-size being larger than 1 μm and having thin spines. It has globular, slightly embracing chambers increasing rapidly in size and 4 chambers in the last whorl. A wide open umbilical aperture, which may be slightly out of its centric position and the size of the aperture, may differ between different 7 genotypes of *G. bulloides*. It has no umbilical lip. The repartition of dextral and sinistral forms of *G. bulloides* seems to be related to temperature, and is balanced in contrast to other species. *G. bulloides* presents frequently Kummerform final chambers.

**Figure 6.** Picture of *Globigerina bulloides.*

*Globigerina bulloides* mainly dwells above the thermocline within the upper 60 m of the water column, and is a non-symbiotic species. Its ecologic preferences are cool and eutrophic waters, usually associated with temperate to sub-polar water masses. The distribution of *G. bulloides* within the surface water column may be modified by hydrographic conditions, the availability of prey or its reproduction strategy. *Globigerina bulloides* is equally characteristic of upwelling environments in lower latitudes similarly due to seasonally enhanced primary production at mid and high latitudes.

*Globigerina bulloides* is an opportunistic species, and often dominates the foraminifer fauna. This fate added to its test flux and sediment assemblage at the ocean floor, made *G. bulloides* to be an important source of geochemical information for paleoceanographic reconstruction.

As an unusual fate for the foraminifera, an important part of *G. bulloides* diet consists of algae. The dissolution susceptibility of *G. bulloides* tests is slightly higher than average among extant species (NOAA, 2017a).

### 1.4.3. *Globorotalia inflata*

It is classified as macroperforate non spinose due to its pore-size being larger than 1 μm and it has no spines. *G. inflata* has a trochospiral test type that exhibits >3–4 chambers in the last whorl. The spiral side is rather flat, and the umbilical side is high convex. The subspherical tetrahedral chambers are scattered by pustules. Pointed pustules occur in front of the aperture. The aperture is bordered by a narrow rim and forms a low arch extending from the periphery towards the umbilicus. During adult ontogeny, pustules grow larger and finally coalesce to form a calcite crust, which is covered by a fine veneer of very small calcite crystals (Hemleben, Spindler, Breitinger, & Deuser, 1985).

*Globorotalia inflata* undergoes gametogenic calcification, and is interpreted to have a monthly reproductive cycle. Due to its regionally high standing stocks and its high fossilization potential, *G. inflata* is an interesting archive in paleoceanography. Fossil tests of *G. inflata* sediment samples are easy to identify due to shiny appearance of this calcite crystals under the microscope light.

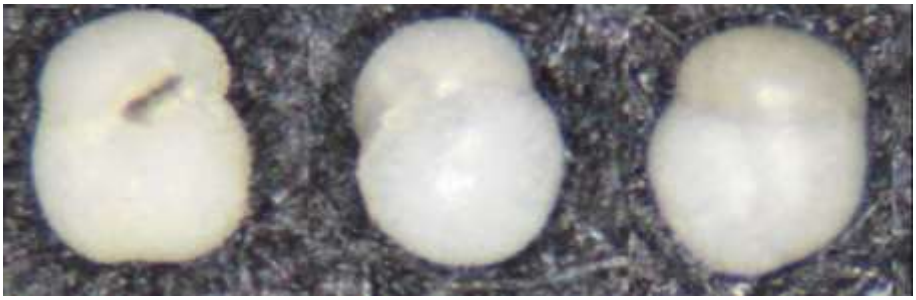

**Figure 7.** Picture of *Globorotalia inflata* specimen in its different sites.

*G. inflata* has two morphotypes, Type I and Type II. Type I is the most common found in the Mediterranean Sea, occurring equatorward of the subpolar front, and has a large aperture in relation to the size of the final chamber (Morard et al., 2011). *Globorotalia inflata* is a dominant species that occurs mainly in transitional environments between subtropical and polar water masses. *Globorotalia inflata* has often been found to occur in the vicinity of hydrographic fronts and eddies, and has hence been interpreted to display an opportunistic behavior limited to mesotrophic conditions in the surface to subsurface water column (Lončarić, van Iperen, Kroon, & Brummer, 2007). It shows relations with sea surface temperature, salinity, and temperature at 200 m but has broad tolerances for these parameters. It has preferences for water masses with little seasonal variation in salinity and shows close relations with winter conditions in the vertical temperature gradient, surface water density, and stratification. In general it becomes abundant under a wider range of physical conditions during summer compared to the winter conditions (NOAA, 2017).

### 1.4.4. *Globorotalia truncatulinoides*

This is classified as macroperforate non spinose due to its large pore-size (>1 μm) and it has no spines. Its trochospiral test type is medium to high conical on the umbilical side, and flat on the spiral side. *Globorotalia truncatulinoides* has 4.5–5.5 tetrahedral chambers in the last whorl. The narrow aperture spans from the rather deep umbilicus towards the periphery, and is bordered by a lip. Pores are distributed over the entire surface. It presents a distinct conical test morphometry, different from all other extant planktic foraminifers. *G. truncatulinoides* has different morphospecies, some right coiling and others left coiling.

**Figure 8.** Picture of *Globorotalia truncatulinoides* specimen in its different sites.

*Globorotalia truncatulinoides* populates the deepest habitat of all extant species, having been sampled alive from the water column below 2000 m water depth (Schiebel & Hemleben, 2005). Is a typically subtropical species which occurs over a broad range of salinities and sea surface temperatures. It prefers areas with little seasonality in salinity in contrast to broad tolerances for seasonal change in sea surface temperatures. Most noteworthy is a distinctly lower tolerance for the vertical temperature gradient and stratification in winter, compared to summer conditions. (NOAA, 2017c).

*Globorotalia truncatulinoides* reproduces once per year in late winter (Bé, Hutson, & Be, 1977). It is speculated that *G. truncatulinoides* generally reproduces in surface waters to provide sufficient food for offspring and for try to avoid competition or predation. The offspring descends in the water column and disperses over the vast expanses of the deep ocean, spending most of the year growing a mature test and producing a calcite crust. In the subtropical ocean towards higher latitudes, *G. truncatulinoides* dwells at decreasing water depths, possibly driven by the availability of food.

The deep habitat of *G. truncatulinoides* makes the species an ideal proxy of surface ocean stratification. The chemical composition of *G. truncatulinoides* tests provides a measure of environmental conditions above and below the seasonal thermocline (Hemleben et al., 1985).

### 1.4.5. *Orbullina universa*

*O. universa* is classified as macroperforate spinose due its large pore-size (>1µm) and spines. It presents ontogeny where its test morphology changes for four to five different stages ending with a spherical test in its terminal stage. It is the only modern foraminiferal species with a spherical test. It has two classes of openings ('pores') distributed over the test wall differentiated by size and function. The large openings act as apertures, and allow exchange of food and other particles including symbionts and cytoplasm (have symbiosis with dinoflagellate). The small openings bear a membrane, and serve the same function as real pores (Spero, 1988).

**Figure 9.** Picture of different specimens of *Orbulina universa.*

*Orbulina universa* is one of the most widely distributed species among planktic foraminifera, whereby its relative abundance hardly ever exceeds 3-4 %. It tolerates wide ranges of ambient water salinity and temperature, and is abundant from tropical to temperate waters (de Vargas, Norris, Zaninetti, Gibb, & Pawlowski, 1999). Test size and porosity of *O. universa* seems to be related to temperature as well as food, and hence the trophic state of surface waters at a regional scale (Be, Harrison, & Lott, 1973). *Orbulina universa* is mostly carnivorous, particularly during its spherical adult ontogenetic stage. Laboratory experiments have confirmed that a larger spherical test growth is related to food richness where calcite is continuously added to the same sphere (Spero, 1988).

According to (André et al., 2014), *Orbulina universa* has three genotypes (I, II, and III) probably related to certain water bodies and trophic conditions, regionally separated by their dominance. The three genotypes differ in the size of pores and apertures. Type III is the genotype found in the Mediterranean; it has small pores and a thinner test wall than Type I but bigger pores than Type II (de Vargas et al., 1999) and is mostly correlated with nutrient rich waters of the western Mediterranean Sea.

As a remarkable fact, reproduction of *O. universa* seems to follow the synodic lunar cycle.

### 1.4.6. Others

The rest of the planktonic foraminifera not belonging to the previous species have been classified as others due to their low abundance or importance in the Mediterranean Sea. These organisms belong to different species and therefore have different ecological requirements. On the other hand, its presence or absence will allow to determine changes in ecologic conditions over time.

# 2. Materials and Methods

## 2.1. The samples

The samples used in this work were obtained during the MedSeA Cruise. The 2013 MedSeA oceanographic cruise was an essential part of the European project “Mediterranean Sea Acidification in a changing climate – MEDSEA” related to Mediterranean Sea acidification and warming, at organismal, ecosystem, and socio-economic impact scales. It went along the Mediterranean Sea sampling sediment cores, plankton tows and aereosol collectors. The major campaign objective was to conduct a comprehensive water column sampling from each of the basins of the Mediterranean Sea. Go to http://medsea-project.eu/ and https://medseaoceancruise.wordpress.com/ for more information.

In May 2013, in the station 23 next to Barcelona’s coast (Latitude: 41.1121 N, Longitude: 2.382 E and Water Depth: 1156 m), the MedSeA Cruise with MC 400 Multi Corer obtained among others Core 1, from 0 until 43.5 cm depth (MUC4-ST23-C1).

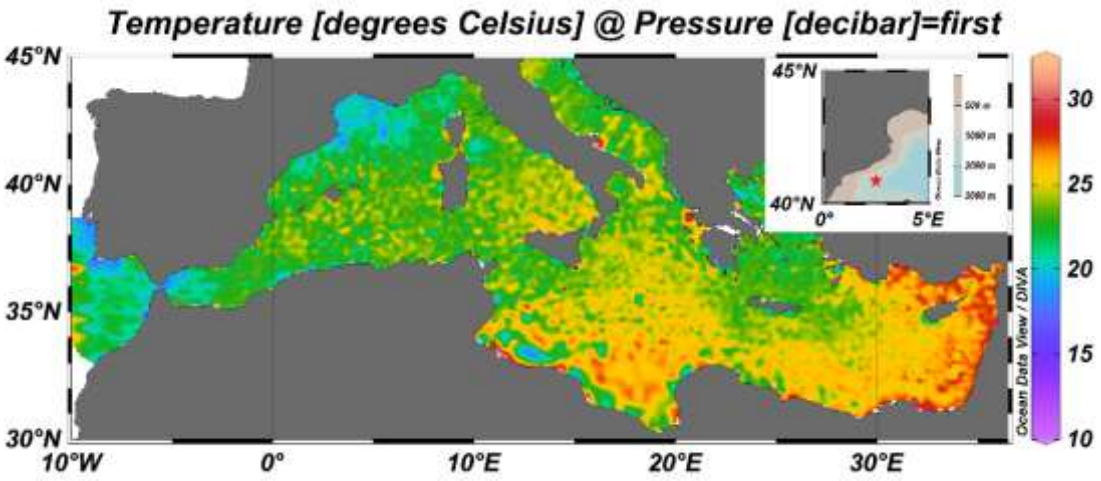


**Figure 10.** Location map of station 23 and Mediterranean basin map with annual average sea surface temperature (SST) today related to surface pressure. Source: Ocean Data View.

The full sediment core **(Figure 12)** was sampled with a 0.5 cm resolution and samples were saved in labeled plastic bags inside a refrigerator. This core contains a sediment archive of the Catalan Sea, according to the age model, between the years CE 2013 to CE 1652. In this work the lower half of the core has been analyzed, with a total of 47 samples between 20 to 43.5 centimeters dated from years CE 1845 to CE 1652.

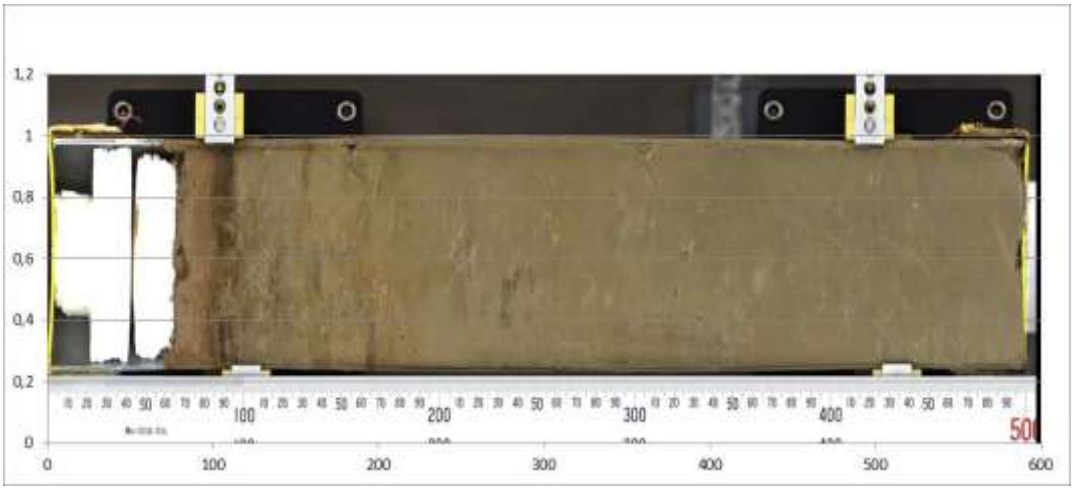


**Figure 12.** Picture of core 1 before being sampled. Source: MedSeA project.

## 2.2. Age model

The age model was based on radionuclide $^{210}$Pb activity determination carrying out the methodology described on Sanchez-Cabeza, Masqué, & Ani-Ragolta, 1998 in order to determinate the geochronology of core 1.

Knowing $^{210}$Pb, the Constant Flux: Constant Sedimentation (CF:CS) model of Krishnaswamy, Lal, Martin, & Meybeck, 1971 was used in order to achieve core dating. This model assumes that both the 210Pb flux and the mass accumulation rates of the deposit are constant. This means that each layer of the record will have the same initial 210Pb activity; therefore, the 210Pb accumulation rate is constant.

Then 210Pb activity profile is plotted on a logarithmic scale against the depth expressed as cumulative dry mass (m); the mean sedimentation rate r (g cm-2 yr -1) can be obtained from the mean slope of the graph (-λ/r) using a least-squares fit procedure. (Garcia, 2011)

Given the shorter half-life of $^{210}$Pb, dating only allows derivation of chronologies for the past 100-150 years so it has not been possible to date the full core. The following age model with isotope $^{210}$Pb was realized for the upper half of the core until almost year CE 1850. Considering a constant sediment rate obtained by (CF:CS) model, it has been possible to date the other part of core.

## 2.3. Foraminiferal composition

To determine the foraminiferal composition a standard procedure was followed: first the samples were dried in the oven at 60ºC for at least 24 hours. Once the samples were totally dried, they were weighed in order to know its bulk mass. Then each of the samples were sieved using a pressurized pump filled with *Elix* water to separate it into two different fractions: larger and smaller than 63 µm.

The fraction larger than 63 µm was oven dried at 80 ºC. Once it was dried, with the help of a paint brush, all the sediment contained in the sieve was placed into a labelled plastic vial with a glass funnel; this process was done using a tray in order to lose the least amount of sample as possible. This fraction contains the foraminifera and is the one that will be used in this work.

The fraction smaller than 63 µm was deposited into labelled plastic bags once the material was settled, the water pipetted out and the sediment oven dried. This material will be used in the near future for doing other experiments.

### 2.3.1. Foraminiferal picking

The picking consists in identify and separate the planktonic foraminifera for the following species: *Globigerinoides ruber* sensu lato, *Globigerinoides ruber* sensu stricto, *Globigerinoides ruber* pink, *Globigerina bulloides*, *Globorotalia* inflata, *Globorotalia truncatulinoides*, *Orbullina universa* and others (other species not very relevant).


**Figure 13.** Own pictures of the different planktonic foraminifera species identified on picking.

An optical microscope, with lightning, was used to identify all shells of different foraminiferal species from the medium fraction. In previous works it was observed that the absolute abundances were stable in the medium fraction (250 - 315 µm), while they were more variable in the small and the large fraction due to the predominance of few species (Anglada, 2016). By using a paint brush, with the help of some water and surface tension, the foraminifera was picked one by one, separated by species and saved in micropaleontological slides.

The rest of the sample larger than 315 µm and smaller than 250 µm goes again into labelled plastic vials with the help of a paint brush and a glass funnel for possible future analysis.

### 2.3.2. Foraminiferal Size-Normalized weight

To know the foraminiferal calcification, Size-Normalized weight (SNW) was determined for the species *G.ruber* sensu lato, *G. ruber* sensu stricto, *G. bulloides*, *G. tuncatulinoides* and *G*. inflata at different resolutions. In the case of both *G. ruber* every sample was measured and the other species were measured every 4 samples the first 20 to 28 centimeters and every 5 samples between 28 centimeters until the bottom of the core.

For each sample and species 10 specimens were selected with the exception of *G. ruber* sensu stricto that as a consequence of its reduced abundance between 5 and 2 specimens were selected.

The foraminifera were weighed using a Sartorius CP2P microbalance in a chamber with stable conditions. The specimens were introduced in an aluminum capsule previously tared, weighed three times and then extracted to weigh the capsule again and correct the possible tare variation. The mass results were obtained doing the average of the three weights (Movellan, Schiebel, Zubkov, Smyth, & Howa, 2012) minus the tare variation divided by the number of specimens weighed. The standard deviation of the mass for each sample was also calculated.

The foraminifera previously weighed were photographed with a camera EOS 650 SLR Canon attached to a Leica Z16 APO lens. Then ImageJ software was used to analyze the images done and determine the surface area for each shell by the minimum ferret calculation in µm and their respective standard deviation (Schneider, C. A., Rasband, W. S., and Eliceiri, 2012).

Once the mass and morphometry were obtained, the SNW was calculated through the methodology of Anglada, 2016 from the following formulas:

**12.** SNW (µg) = C + [C*[100-(100/B)*A]/100]

In this formula A represents the minimum ferret in µm, B the average of all the minimum ferrets of the whole core from each species in µm and C the specimen average mass in µg.

Apart from SNW it is also needed the cumulative standard deviation that is calculated as follows:

**13. C**um std dev (%) = [(100/C)*D] + [(100/A)*E]

Where D represents the standard deviation of the average mass and E the standard deviation of the minimum ferret (Anglada, 2016)**.**

# 3. Results

## 3.1. Age model

From the constant sedimentation rate of 0,119 (cm/year), obtained through (CF:CS) model by $^{210}$Pb dating, and assuming that the uppermost 0 cm span the last 2013 years, it was possible to date core 1. Where according to these calculations, the last 43 cm span the last CE 1652 years.

## 3.2. Foraminiferal composition

### 3.2.1 Foraminiferal abundance

Based on the results obtained from the foraminiferal picking it is possible to represent absolute and relative abundances. These indicate that in both plots *G. bulloides* was the most dominant species followed by *G. infata*, others, *G. truncatulinoides* and *G. ruber* sensu lato. The less abundant species were *G. ruber* sensu stricto, *Orbullina universa* and *G. ruber* pink. **(Table 1 and Table 2)**

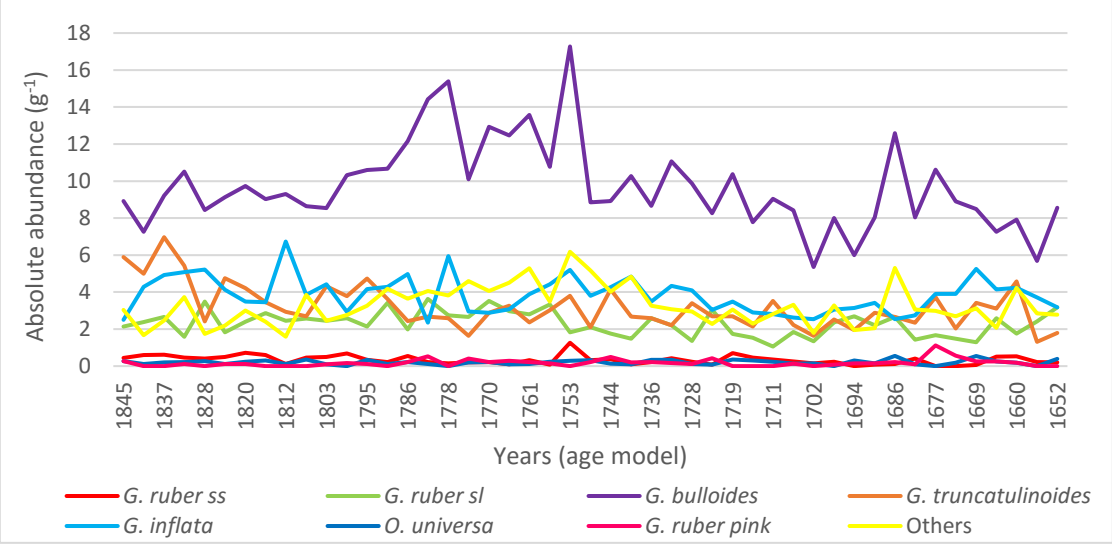


**Figure 14.** Absolute abundance of all the picked species for the half bottom part of core 1.

An increasing trend in most of all foraminiferal absolute abundances is seen until year 1845 with the exception of *G. inflata*, *G. ruber* sensu lato and *Orbullina universa*. In the cases of *G. ruber* sensu lato and *Orbullina universa,* they have the same percentage variation. **(Table 1)**

In the following results, the percentage of variation was done to quantify the tendency and the difference between the first to the last value recorded. Negative values in the percentage of variation means an increase and negative values a decrease of the studied parameters.

| Species | Total Ab. ab ($g^{-1}$) | Variation (%) |
|---|---|---|
| *G. bulloides* | 456.44 | -4.17 |
| *G. inflata* | 180.61 | 27.35 |
| Others | 153.15 | -8.23 |
| *G. truncatulinoides* | 149.23 | -69.61 |
| *G. ruber* sl | 108.21 | 48.58 |
| *G. ruber* ss | 15.76 | -55.43 |
| *O. universa* | 9.49 | 48.58 |
| *G. ruber* pink | 8.06 | -100 |

**Table 1.** Foraminiferal species ordered from highest to lowest total absolute abundance and their respective percentage of variation.

Following that, **Figure 14** represents in three separated plots according to the species abundance, more detail over time. **(Figure 15)**: **(a)** represents the most dominant specie according to the results, *G. bulloides,* which is slightly variable in absolute abundance, with some important ups and downs, has increased by 4.17%. Its highest value was at CE 1753 (17.28 g) and the lowest at CE 1702 (5.36 g); in **(b)** are represented the most abundant species below *G. bulloides.* We can see a big increase of *G. truncatulinoides* absolute abundance of a 69.61% and a considerable decrease of a 48.58% on *G. ruber* sensu lato and a decrease of a 27.35% on *G. inflata*. Others has the most stable results with a slight increase of 8.23% in its absolute abundance while *G. truncatulinoides* was the most unstable with many ups and downs and a huge increase starting from year CE 1828. The most outstanding feature of this graph can be observed from year 1812 where the absolute abundance of others is surpassed by the one of *G. truncatullinoides* and where later it also exceeds the absolute abundance of *G. inflata* in the year 1832; in **(c)** are represented the less abundant species according to the obtained results. There was an almost 50% abundance decrease in *Orbullina universa* with the most stable results, and more than a 50% increase on *G. ruber* sensu stricto abundance with the less stable results of the three species. It was also remarkable a huge peak in *G. ruber* sensu stricto absolute abundance on year CE 1753 before one of the lowest abundance peaks. The percentage of change in *G. ruber* pink was -100% due to no specimens in the first and the last years. During the core time interval, there were years where specimens are also not found in the samples, apart from that, the results were quite stable with the exception of a big abundance peak on year CE 1677. Still not having a clear percentage of variation, the trend line shows that its absolute abundance has dropped.

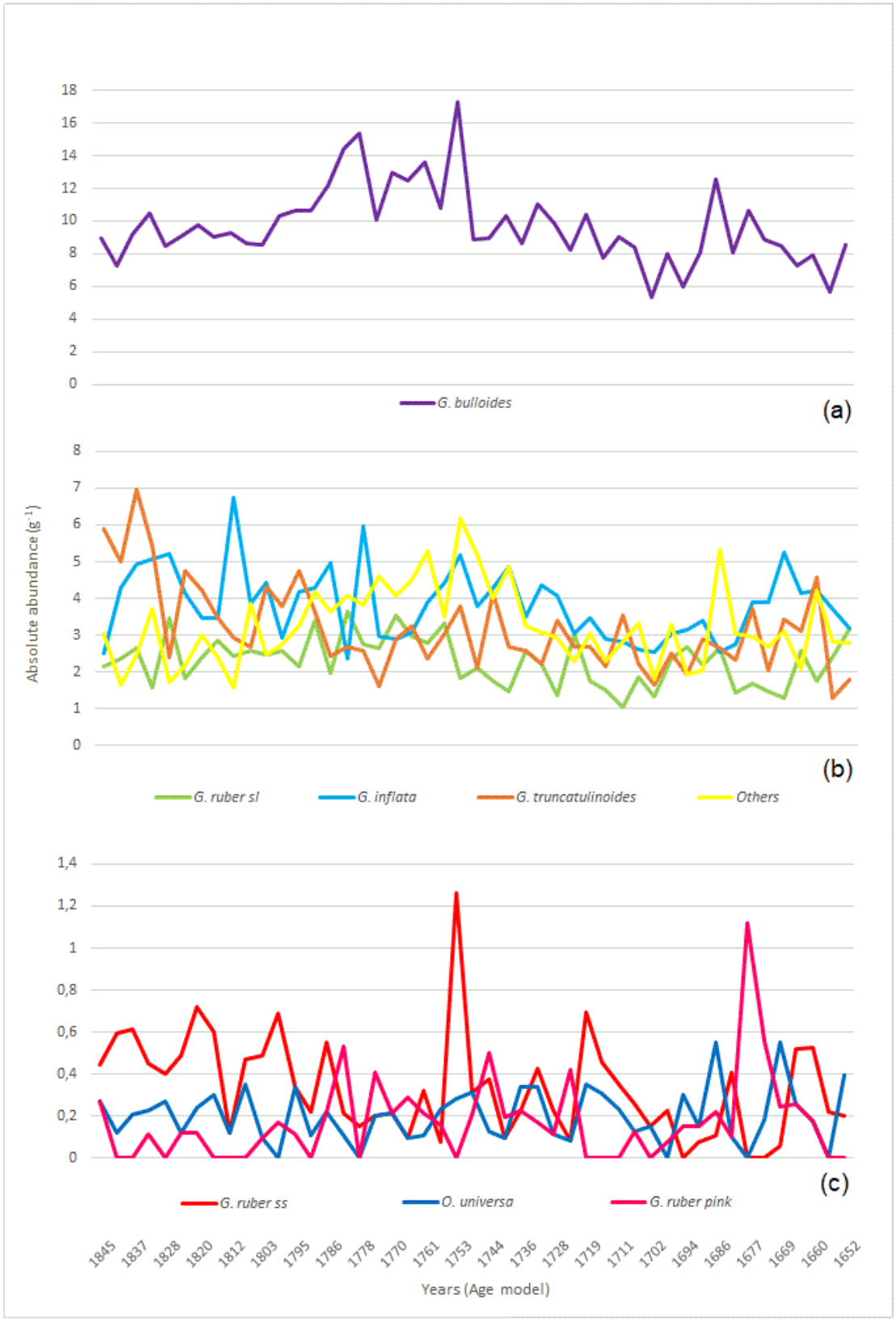


**Figure 15.** Absolute abundance results separated in three: *G. bulloides* absolute abundance **(a)**, the absolute abundance of the most abundant species bellow *G. bulloides* **(b)** and the less abundant species **(c)**.

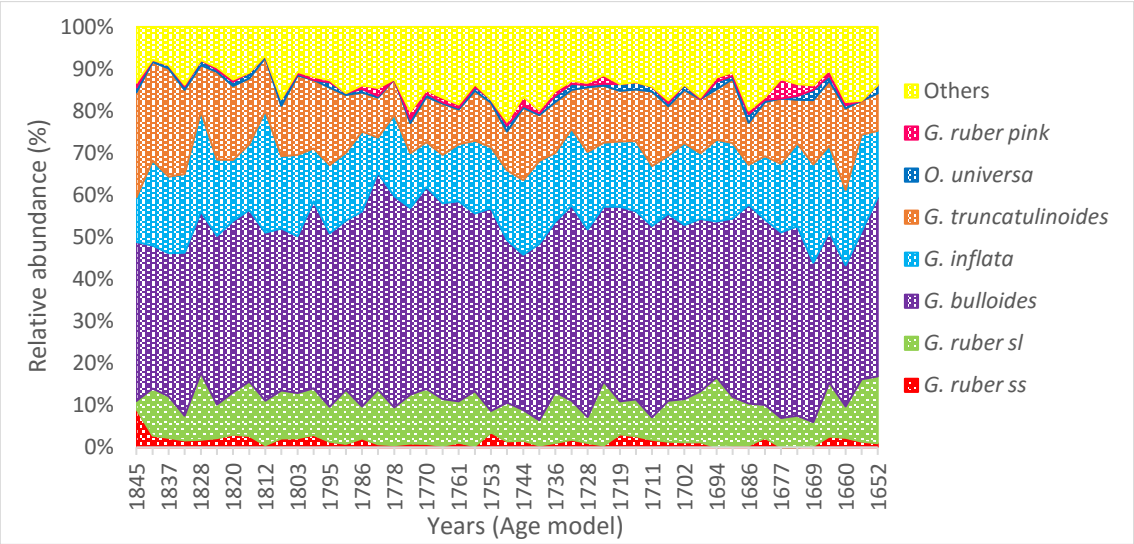


**Figure 16.** Relative abundance of the half bottom part of core 1.

The plot, confirms *G. bulloides* as the most abundant specie of the core with a relative abundance of 41.94%. The rest of the species represent a 58.06% of the total. *G. inflata* was the second most abundant with a 17.20%, being a big difference compared to *G. bulloides* **(Table 2)**. The relative abundance has experienced a decrease in the majority of the species as it is going to recent records, where *G. bulloides* and others have positive values on the percentage of variation in contrast to previous absolute abundance results. However *G. truncatulinoides*, *G. ruber* sensu stricto and G. ruber pink increase. *G. ruber* sensu lato and *Orbullina universa* have also the same percentage variation but different results with absolute abundance. Both species had a 73.60%, the highest percentage of decrease on relative abundance. *G. truncatulinoides* has the biggest increase with a 64.49% on relative abundance like in absolute abundance.

| Species | Relative ab. (%) | Variation (%) |
|---|---|---|
| *G. bulloides* | 41.94 | 11.97 |
| *G. inflata* | 17.20 | 48.80 |
| Others | 14.09 | 3.96 |
| *G. truncatulinoides* | 13.51 | -64.49 |
| *G. ruber* sl | 10.01 | 73.60 |
| *G. ruber* ss | 1.60 | -47.92 |
| *O. universa* | 0.90 | 73.60 |
| *G. ruber* pink | 0.74 | -3,20 |

**Table 2.** Foraminiferal species ordered from highest to lowest total relative abundance and their respective percentage of variation.

## 3.2.2 Size-Normalized weight results

### 3.2.2.1 Mass results

From weighing foraminifera in the microbalance it was able to obtain the specimen Average Mass per sample for the species *G. ruber* sensu stricto, *G. ruber* sensu lato, *G. bulloides*, *G. inflata* and *G. tuncatulinoides*.

*G. bulloides* mass is the most stable of all of them meanwhile *G. ruber* sensu stricto is the less stable with two highest peaks on the years 1681 and 1736. *G. tuncatulinoides* and *G. inflata* mass became superposed on year 1736 and *G. ruber* sensu lato mass was stable in a range of values but with lots of up and downs.

In this plot the results are in inverse order due to *G. inflata* is the heaviest specie and *G. bulloides* is the lightest specie and by this way the representation becomes more accurate.

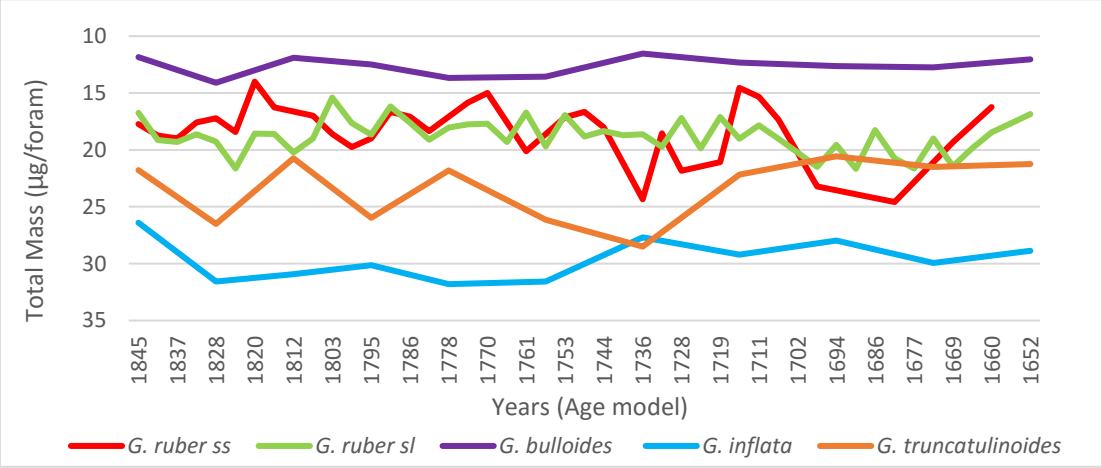


**Figure 17.** Specimen average mass of the half bottom part of core 1.

As it is going more recent records *G. ruber* sensu lato, *G. bulloidesand* and *G. inflata* mass decreases meanwhile *G. ruber* sensu stricto and *G. tuncatulinoides* increases. The mass of *G. inflata* is the one that has decreased more with 9.34% and the mass of *G. ruber* sensu stricto is the one that has had the biggest increase of 8.52% of its mass. **(Table 3)**.

| **Species** | *G. ruber* ss | *G. ruber* sl | *G. bulloides* | *G. inflata* | *G. tuncatulinoides* |
|---|---|---|---|---|---|
| **Variation (%)** | -8,52 | 0,80 | 1,69 | 9,34 | -2,37 |

**Table 3.** Percentage of variation from the different specimens mass results of the half bottom core 1.

### 3.2.2.2 Foraminiferal Size-Normalized weight

Normalizing the specimens weigh according to its dimensions, minimum ferrets, and its respective standard deviations was possible to proceed with SNW formulas and obtain the following results:


**Figure 18.** Size-Normalized weight of the half bottom core 1; **(a)** for all the species, **(b)** *G. ruber* sensu stricto, **(c)** *G. ruber* sensu lato, **(d)** *G. bulloides*, **(e)** *G. inflata* and **(f)** *G. tuncatulinoides* with its accumulate standard deviation.

As in the previous mass results *G. inflata* has biggest SNW because its high test calcification rate, *G. bulloides* have the lowest and the most stable SNW results and *G. ruber* sensu stricto is the most instable with the highest values in accumulate standard deviation.

Comparing SNW results with mass confirms that the results were realized properly besides the big accumulate standard deviation of some species. There were only slight differences in *G. ruber* sensu stricto and *G. tuncatulinoides* which have reduced its instability and there was no *G. tuncatulinoides* superposition to *G. inflata* at year CE 1736. Conversely *G. ruber* sensu lato, *G. bulloides* and *G. inflata* increases its instability.

During the pre-industrial times *G. tuncatulinoides, G. ruber* sensu lato and *G. inflata* had experienced a decrease on its SNW while conversely *G. ruber* sensu stricto and *G. bulloides* increases. *G. tuncatulinoides* was the specimen with the highest decrease of a 10.74% whereas that *G. ruber* sensu sricto has a 10.11% of increase. **(Table 4)**

| **Species** | *G. ruber* ss | *G. ruber* sl | *G. bulloides* | *G. inflata* | *G. tuncatulinoides* |
|---|---|---|---|---|---|
| **Variation (%)** | -10.11 | 9.05 | -2.20 | 4.56 | 10.74 |

**Table 4.** Percentage of variation from the different SNW specimens results of the half bottom core 1.

# 4. Discussion

This chapter has been divided into two parts: in the first one the results previously shown were plotted together with those made by obtained by *Griselda Anglada* in order to have core 1 completed; the second part has consisted to compare physical factors that may have altered foraminiferal behavior with core 1 results. Thereby, they allow to understand the results presented below related to the objectives of this project.

## 4.1 Core 1 results

In order to obtain a representative and comparable record of the sample analyzed. It has been necessary to incorporate core 1 upper part results, obtained by *Griselda Anglada*, to the previously shown results. Once both came together, core 1 was finally completed. This allows the possibility to compare the foraminiferal behavior over the entire core and the different changes on their dynamics between post-industrial and pre-industrial $CO_2$ levels.

### 4.1.1 Core 1 foraminiferal abundance

From foraminiferal picking it was possible to determine absolute and relative abundances. Both indicate that *G. bulloides* was the most dominant species meanwhile *G. ruber* sensu stricto, *Orbullina universa* and *G. ruber* pink were the less abundant **(Table 5 and 6).**

Comparing the total abundances of the whole core with those of bottom part, a change in the abundance order can be observed between different species. *G. truncatulinoides* abundance has increased considerably after year CE 1812, surpassing others in both abundances and in the case of relative abundance has also surpassed *G. inflata* **(Tables 1, 2, 5 and 6).**

This shows the remarkable importance of representing the entire core results. If only the results obtained in this work had been plotted, these would not be representative and therefore its discussion would have been somewhat misleading.

In core 1, *G. bulloides* has the highest total absolute abundance followed by *G. inflata, G. truncatulinoides,* others, *G. ruber* sensu lato and the less abundant species previously mentioned. Dividing the results through pre-industrial and post-industrial CO2 concentrations, it can be seen that post-industrial total absolute abundances of *G. bulloides*, *G. inflata, G. truncatulinoides* and *Orbullina universa* species had greater values than those of the previous period, with the highest increase of a 15.3% for *G. truncatulinoides*.

To know the variation of absolute abundance results during over time, the percentage of variation has been calculated for core 1. As it is going to recent records, the absolute abundance of the species *G. inflata*, *G. ruber* sensu stricto and *G. truncatullinoides* have increased. The latter is the one that has increased in greater number its absolute abundance, by 56.21%. Meanwhile *G. bulloides,* others and *G. ruber* sensu lato decreased. It is necessary to emphasize the considerable drops of 120.37% and 4181.51% of these last two species. A considerable reduction on *G. ruber* sensu lato absolute abundance has happened, which was one of the most abundant species to become one of the species less abundant of the core. *Orbulina universa* and *G. ruber* pink percentage was not possible to be calculated due to the absence of specimens.

Differences on absolute abundance variability between post-industrial and pre-industrial levels have shown that after year 1850 a fall on absolute abundance has happened, with the exception of *G. ruber* sensu stricto. On the contrary, the same does not happen during the period analysed before 1850, when the absolute abundances of *G. bulloides, G. truncatullinoides,* others and *G. ruber* pink augmented as well as *G. ruber* sensu stricto does **(Table 5)**.

Although the total absolute abundance of the post-industrial period is greater than in pre-industrial period, the percentage of variation indicates a decrease in absolute abundance during post-industrial period. This fact is due to the great increase of the absolute abundance from the year 1849 but from year 1971 the abundance has diminished considerably. So the average of absolute abundance values has hidden this decline. The significant decrease in abundance especially from year 1971 indicates a change of the ecologic conditions.

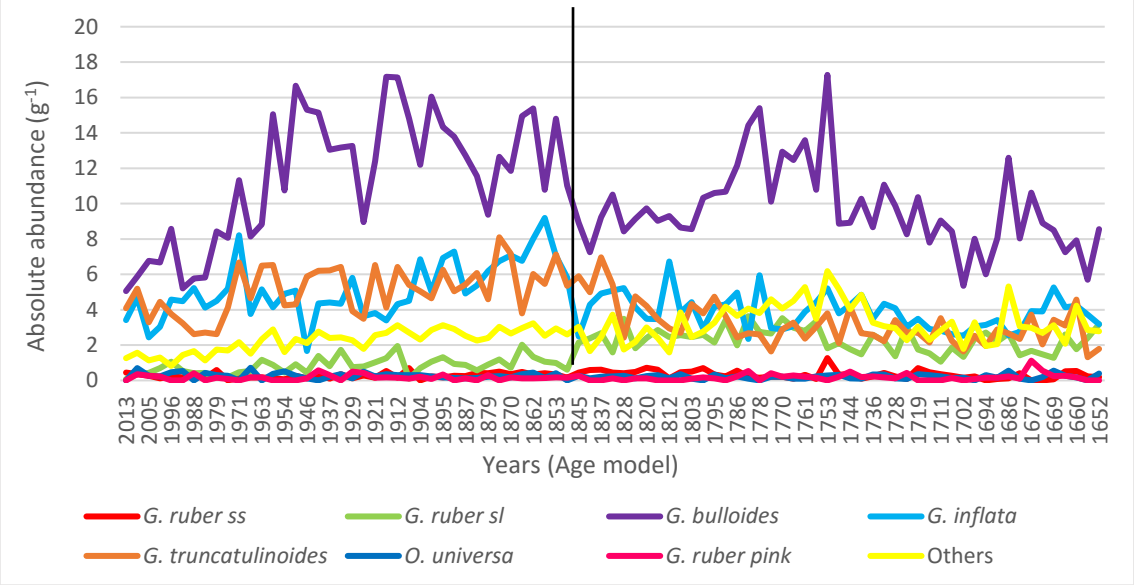


**Figure 19.** Absolute abundance of core 1 picked species with a line on year CE 1805 that separate the results done by Anglada, 2016 (post-industrial levels) from those previously obtained (pre-industrial levels).

| Species | Total abs. Ab. ($g^{-1}$) | Total abs. Ab. ($g^{-1}$) post-ind. levels | Total abs. Ab. ($g^{-1}$) pre-ind. levels | Variation (%) core 1 | Variation (%) post-ind. levels | Variation (%) pre-ind. levels |
|---|---|---|---|---|---|---|
| *G. bulloides* | 915.18 | 458.74 | 456.44 | 69.21 | 117.91 | -4.17 |
| *G. inflata* | 386.89 | 206.29 | 180.61 | -6.92 | 70.02 | 27.35 |
| *G. truncatulinoides* | 352.73 | 203.50 | 149.23 | -56.21 | 30.97 | -69.61 |
| Others | 242.89 | 89.74 | 153.15 | 120.37 | 105.81 | -8.23 |
| *G. ruber* sl | 141.38 | 33.17 | 108.21 | 4181.51 | 723.24 | 48.58 |
| *G. ruber* ss | 26.41 | 10.65 | 15.76 | -55.40 | -65.70 | -55.43 |
| *O. universa* | 20.05 | 10.57 | 9.49 | - | - | 48.58 |
| *G. ruber* pink | 14.28 | 6.21 | 8.06 | - | - | -100 |
| **Total specimens** | 2099.81/ **87 samples** | 1018.86 / **40 samples** | 1080.95 / **47 samples** | 40.04 | 79.15 | -14.41 |
| **Total spe./sample** | 24.14 | 25.4715 | 22.998 | | | |

**Table 5.** Foraminiferal species ordered from highest to lowest total absolute abundance with their respective percentage of variation for the whole core 1, post-industrial levels total absolute abundance and percentage of variation (upper part results) and pre-industrial levels total absolute abundance and percentage of variation (bottom part results), **(Table 1)**.

As in the previous chapter the absolute abundance plot, now for the whole core **(Figure 19),** has been separated by three to see in more detail the absolute abundance results over time **(Figure 20)**: in **(a)** was represented *G. bulloides,* the most dominant species. Although it shows considerable variation in absolute abundance, this plot shows the existence of a cyclicity every 180 years approximately. The highest absolute abundance result was on year CE 1752 (17.28 g). From the year 1841 the results show a considerable increase, that before 1971 decreases to the lowest values recorded in the core on year CE 2013 (5.052 g). Even so the tendency line shows a positive increase on the abundance; in **(b)** were represented the most abundant species below *G. bulloides.* In older records the absolute abundances of the four species were closer but going to actuality its results became more and more separated and divided in two tendencies; where *G. inflata* and *G. truncatullinoides* had greater values, others and *G. ruber* sensu lato decrease considerably. The tendencies of G. *inflata* and *G. truncatullinoides* abundances were similar to *G. bulloides,* which after the year 1841 increased considerably and later year 1971 diminished but in this case the most recent values were not lower than the first recorded. A reduction in others abundance means a change on ecological conditions. And *G. ruber* sensu lato was the species with the biggest instability, which has the highest drop on its absolute abundance from year 1845 to the present day. These prominent changes suggest that there has been a variation in ecological conditions in the studied area from approximately year 1840 until today; in **(c)** were represented the less abundant species. The absolute abundances of *Orbullina universa*

and *G. ruber* pink had experienced a decrease from past years to actuality taking into account the difference between the first to the last values recorded, but in the case of *O. universa* the values tendency shows an increase on its absolute abundance conversely to *G. ruber* pink. There is a significant difference between *G. ruber* sensu stricto values that increased positively and have the highest stability compared to the rest of species of the plot. However, by looking at the values trend we can see a very slight decrease of them. The three species coincide on a fall of their abundance in the year 1849. And finally, the decrease on *G. ruber* pink absolute abundance all over the plot indicates salinity decrease.

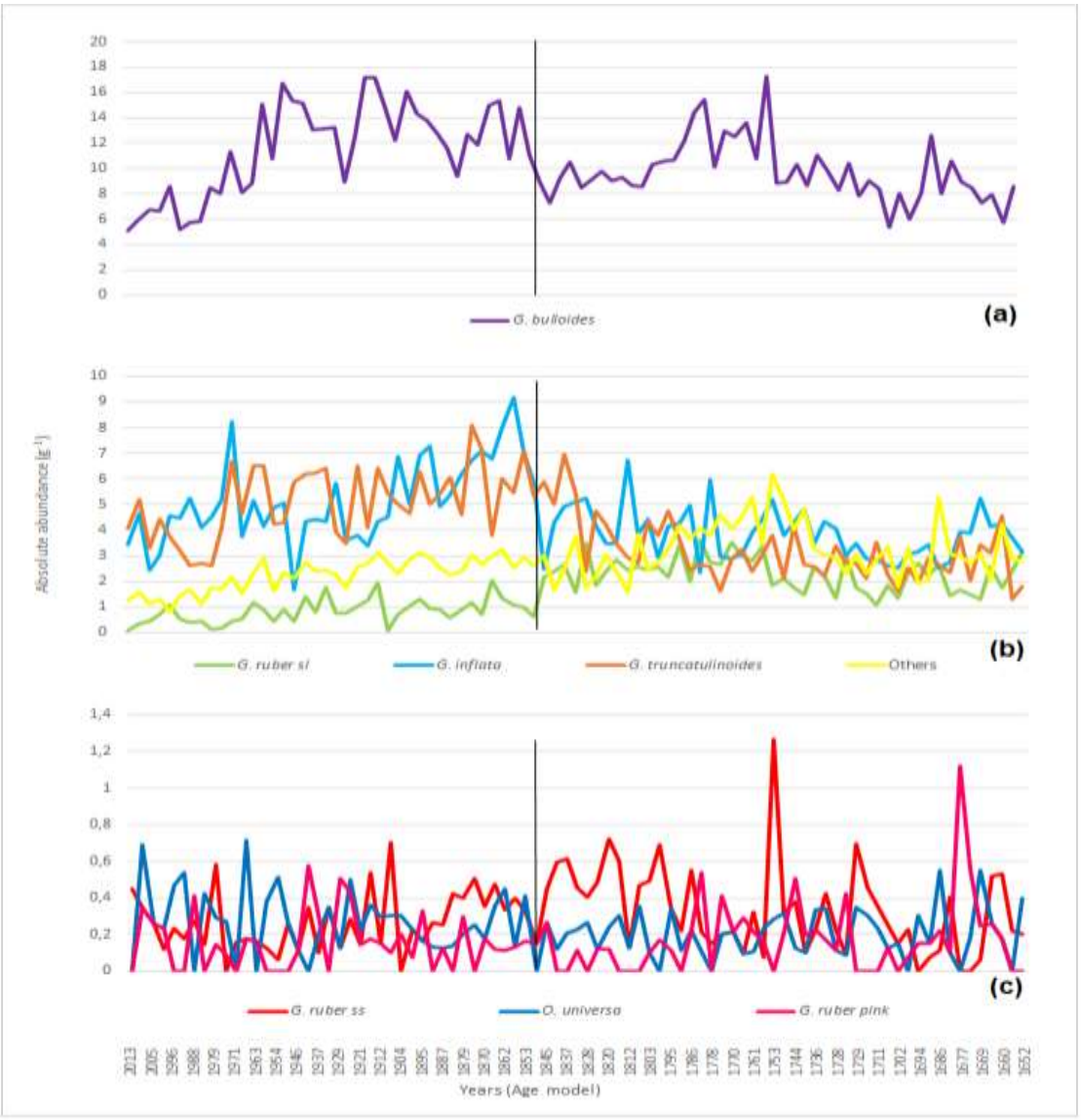


**Figure 20.** Absolute abundance results of core 1 separated in tree: *G. bulloides* absolute abundance **(a)**, the absolute abundance of the most abundant species below *G. bulloides* **(b)** and the less abundant species **(c)**. Each plot has a line on year CE 1805 that separates the results done by Anglada, 2016 (post-industrial levels) from those previously obtained (pre-industrial levels).

As it is previously said *G. truncatulinoides* becomes the species with second highest total relative abundance surpassing *G. inflata*. Differences between pre-industrial and post-industrial total relative abundance follows the same dynamic as absolute abundance.

The most remarkable fact on **Figure 21**, is the big fall of *G. ruber* sensu lato relative abundance that has happened after year 1845 until the present day, while others, *G. ruber* sensu sricto and *G. ruber* pink also decrease but not too considerably as the first. Nevertheless *G. bulloides, G. inflata, G. truncatulinoides* and *O. universa* relative abundances have increased from pre-industrial to post-industrial times. **(Table 6)**

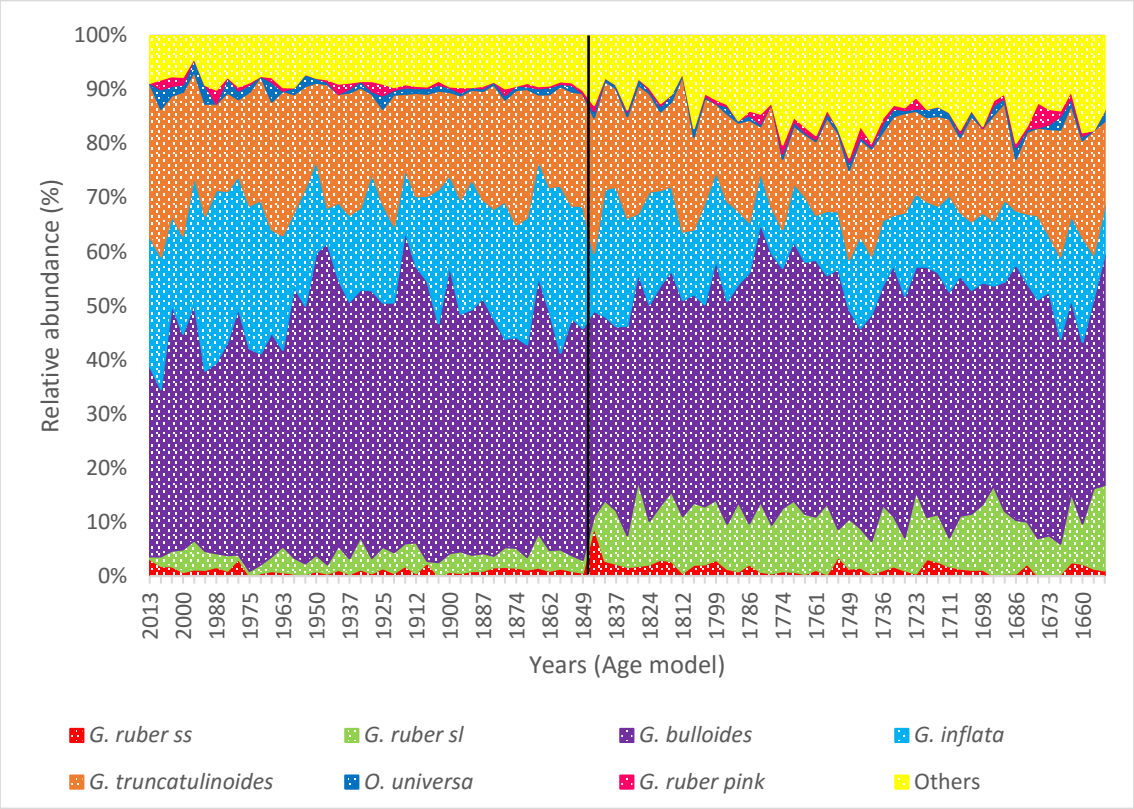


**Figure 21.** Relative abundance of core 1 picked species with a line on year CE 1805 that separate the results done by Anglada, 2016 (post-industrial levels) from those previously obtained (pre-industrial levels).

About the percentage variation of core 1, the most outstanding value is the 2957.43 % of reduction on *G. ruber* sensu lato relative abundance. A reduction of a 57.37 % in others relative abundance and a reduction of a 20.84% in *G. bulloides* relative abundance are also significant. The rest of the species show a notable increase where *G. ruber* sensu sricto has the highest value of a 68.15 % closely followed by *G. inflata* with an increase of 62.61 %.

A 359.52 % of variation on *G. ruber* sensu lato relative abundance post-industrial levels is the most outstanding value of the results obtained, indicating a large decrease in its abundance as the years are closer to 2013. The values of the three different percentage of variation follow similar dynamics between them, except *G. inflata* that its percentage is negative on pre-industrial levels and positive on post-industrial levels, meaning that first its abundance decreases and then increases until recent times. The decrease on *O. universa* shows a change on ecological conditions.

| Species | Total relative Ab. (%) | Total rel. Ab. (%) post-ind. levels | Total rel. Ab. (%) pre-ind. levels | Variation (%) core 1 | Variation (%) post-ind. levels | Variation (%) pre-ind. levels |
|---|---|---|---|---|---|---|
| *G. bulloides* | 43.05 | 44.34 | 41.94 | 20.84 | 21.64 | 11.97 |
| *G. truncatulinoides* | 18.58 | 20.21 | 13.51 | -44.41 | -26.89 | -64.49 |
| *G. inflata* | 16.80 | 20.67 | 17.20 | -62.61 | -5.10 | 48.80 |
| Others | 11.62 | 8.73 | 14.09 | 57.37 | 14.88 | 3.96 |
| *G. ruber* sl | 6.86 | 3.15 | 10.01 | 2957.43 | 359.52 | 73.60 |
| *G. ruber* ss | 1.37 | 1.10 | 1.60 | -68.15 | -80.85 | -47.92 |
| *O. universa* | 1.01 | 1.15 | 0.90 | - | - | 73.60 |
| *G. ruber* pink | 0.70 | 0.65 | 0.74 | - | - | -100 |

**Table 6.** Foraminiferal species ordered from highest to lowest total relative abundance with their respective percentage of variation for the whole core 1, post-industrial levels percentage of variation (upper part results) and pre-industrial levels percentage of variation (bottom part results, **Table 2**).

### 4.1.2 Core 1 foraminiferal size-normalized weight

Size-normalized foraminiferal shell weight is used as a proxy for past carbonate ion concentration in seawater, assuming that reduced carbonate ion concentration and pH lead to lower calcification rates and lighter, thinner shells (Pak, Clayman, Weaver, Schimmelmann, & Hendy, 2011). What is intended to be done in this chapter is to determine if core 1 SNW results suggested that the uptake of anthropogenic $CO_2$ and ocean acidification over the last century has resulted in lower shell weight.

Cumulative standard deviation was not possible to plot because of problems on both core 1 measurements. The results first obtained have had to be correlated using a regression line in order to be comparable. So the results of chapter 3.2.2.2 are not the same as those shown below.

According to **Figure 22**, *G. bulloides* was the species with the most stable SNW and *G. ruber* sensu sricto has the highest instability. The most relevant of this graph, apart from the low peak of *G. ruber* sensu stricto SNW on year 2000, the fall of *G. ruber* sensu lato SNW after year CE 1963 and the two periods where *G. truncatulinoides* superposes *G. inflata*.

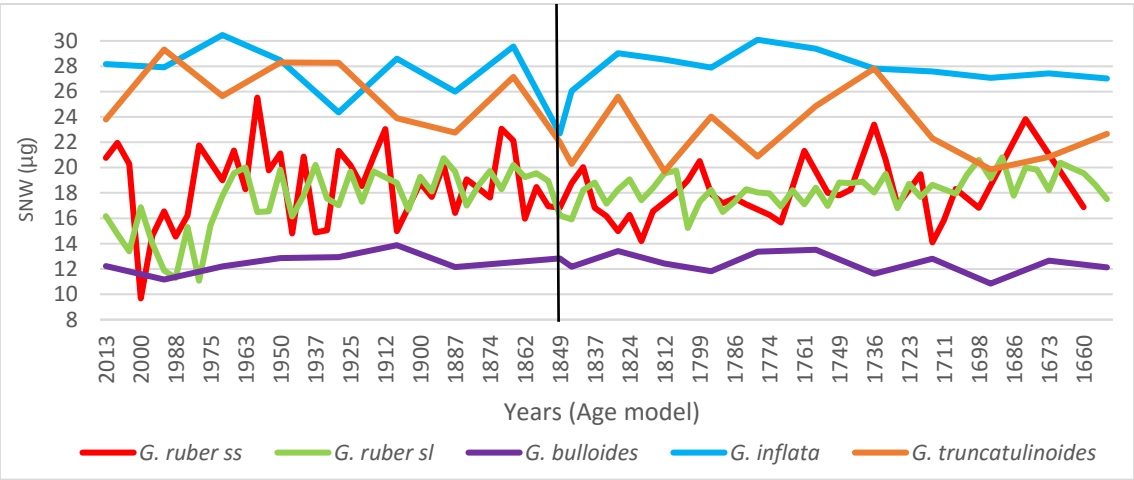


**Figure 23.** Size-normalized weight of the whole core 1.

In **Figure 23** each species has been plotted separately in order to do a more detailed analysis of the results and compare them between post-industrial and pre-industrial levels. It must be taken into account that after year 1845 the SNW of all the species have changed their tendency: Referred to **(a)** The overall results show that since the first recorded years *G. ruber* sensu sricto had experienced a considerable increase on its SNW of an almost 19%, and is the highest respect of the rest analysed species. This increase was more considerable in post-industrial times. Conversely in this period *G. ruber* sensu sricto SNW had experienced its lowest results between

the year CE 1979 to CE 2005 and especially in the year 2000; the inverse situation has happened on **(b),** while over the years *G. ruber* sensu lato SNW decreased considerably becoming the analysed species with the highest decrease of 8.35%. During pre-industrial period was decreased the most, although it must also be highlighted a fall on SNW from year CE 1963 until the last recorded year, with a decrease of almost 24%. Compensated by a previously growth of almost 20%; in the case of **(c)**, besides *G. bulloides* anomaly low result on year 1694 its SNW had grown through the pre-industrial period and in the post-industrial period until a decline in year CE 1908. And on year CE 1992 increases again until year 2013. As a result of all these variations *G. bulloides* SNW has increased almost 1%; as it can be seen on plot **(d)**, *G. inflata* SNW during pre-industrial period was quite stable until its most considerable fall between years CE 1828 to CE 1849. Thereafter, the results become more irregular and variable until year CE 1971, the highest recorded value. Then it falls again in year CE 1992 and then increases slightly until 2013. The most recent results indicate that *G. inflata* SNW could return to the previous stability of the oldest years. Although there is a difference between them, indicating a positive growth of more than 4% in *G. inflata* SNW; finally on **(e)**, *G. truncatulinoides* SNW results follows the opposite tendency of those of *G. bulloides.* During pre-industrial period the results were so variable and decreasing despite a high value on year 1736. From the year CE 1845 the results have followed a positive trend until year CE 1992 where these declined again until 2013. Even so, the last value is higher than the last recorded and therefore there has been a growth in *G. truncatulinoides* test calcification.

| **Species** | *G. ruber* ss | | *G. ruber* sl | | *G. bulloides* | | *G. inflata* | | *G. tuncatulinoides* | |
|---|---|---|---|---|---|---|---|---|---|---|
| **Variation (%)** | -18.82 | | 8.35 | | -0.98 | | -4.05 | | -4.75 | |
| **Post / Pre ind. levels** | -18.97 | -10.12 | 0.33 | 9.93 | 4.88 | -0.53 | -19.42 | 3.75 | -7.56 | 11.69 |

**Table 7.** Percentage of variation from SNW results of core 1, post-industrial and pre-industrial levels.

The results show *G. ruber* sensu lato as the only species in which its shell weight has been reduced, especially after year 1963. Conversely *G. truncatulinoides* is the species for which shell weight increases the most. Both species have similar $r^2$ values. Knowing that *G. ruber* sensu lato is the shallowest species and *G. truncatulinoides* is the deepest, meanwhile the rest of species, the intermediate ones, have low significant $r^2$ values. In conclusion *G. truncatulinoides* is the more calcified with higher SNW in [$CO_3^{2-}$] supersaturated seawater, so it is possible to hypothesise about a change in the water column conditions and an important penetration of atmospheric CO2 in the superficial sea waters.

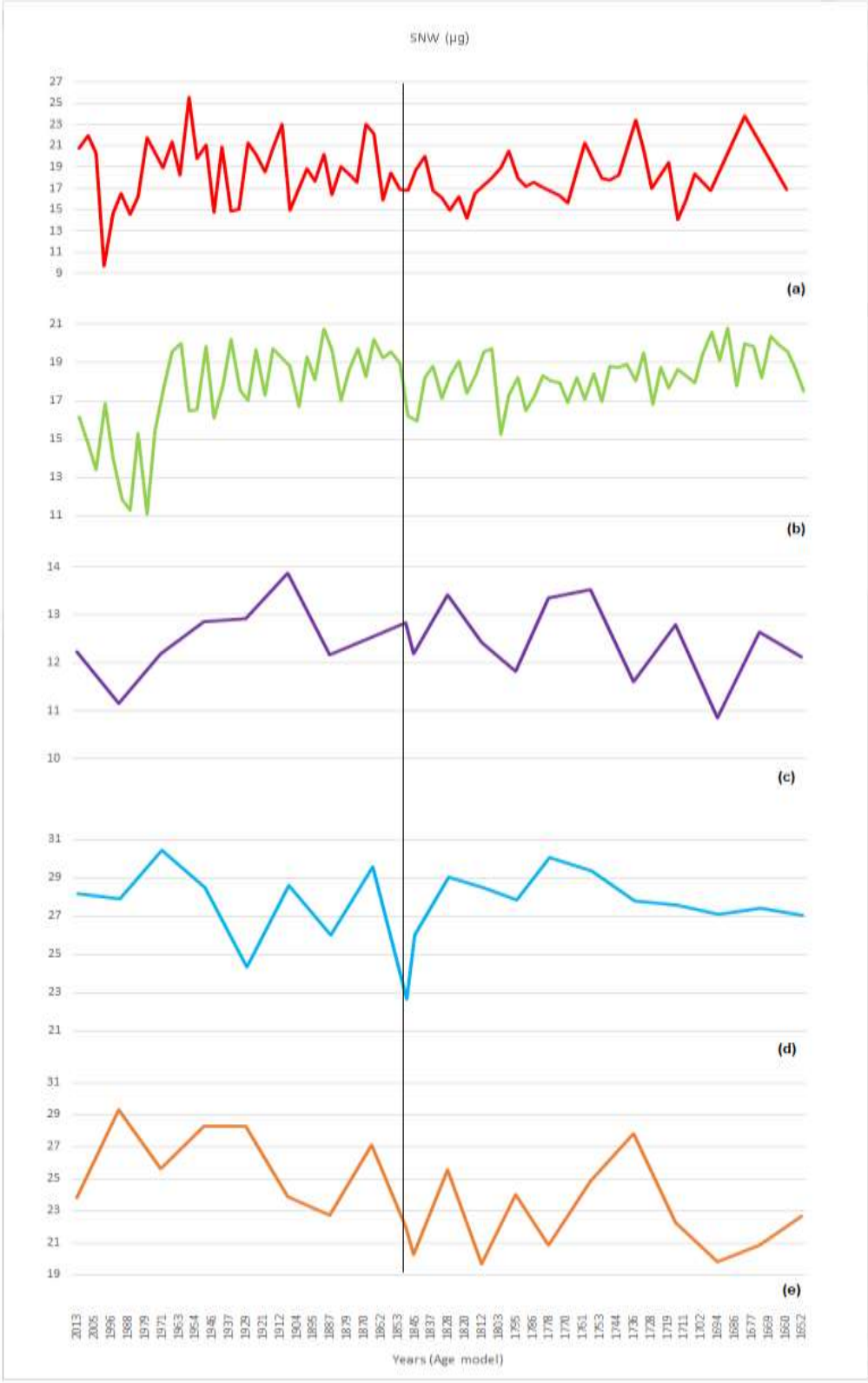


**Figure 24.** Size-Normalized weight of the species: **(a)** *G. ruber* sensu stricto, **(b)** *G. ruber* sensu lato, **(c)** *G. bulloides,* **(d)** *G. inflata* and **(e)** *G. tuncatulinoides* with a line on year CE 1805 that separate the results done by *Anglada, 2016* (post-industrial levels) from those previously obtained (pre-industrial levels).

## 4.2 Core 1 related to physical factors

Yearly physical factors from the studied period may affect the analyzed foraminiferal species, and were summarized in order to understand the values obtained and their effects on the species dynamics. These are: $CO_2$ concentration (ppm), Sea Surface Temperature (Cº), North Atlantic Oscillation (NAO) and Historical Total Solar Irradiance (W/m$^2$).

### 4.2.1 Factors to take into account on discussion

#### 4.2.1.1 $CO_2$ concentration

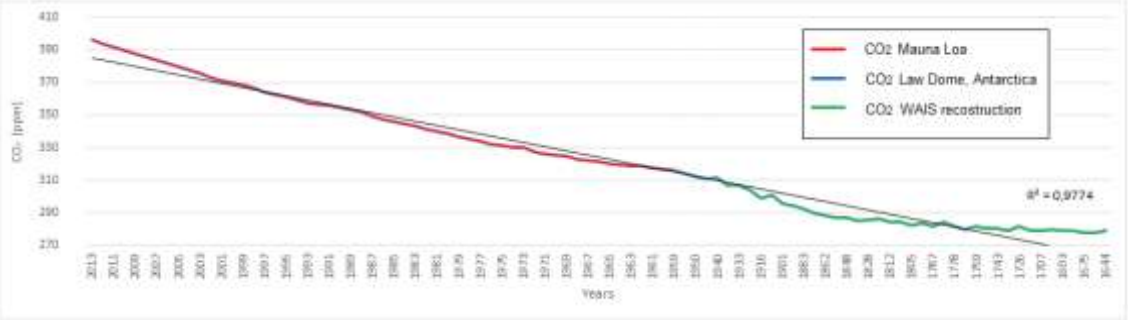


**Figure 24**. Annual $CO_2$ concentration of the studied period (2013-1652). As it can be seen on the legend, the values obtained from Mauna Loa Observatory were on red colour, the Law Dome were represented in blue colour and the values from WAIS reconstruction by Ahn et al., 2012 were in green colour.

Three $CO_2$ records from different sources have been used in order to obtain an accurate $CO_2$ record for the studied period. The most recent values **(red curve)** are direct measurements of annual $CO_2$ in the atmosphere that came from Mauna Loa Observatory, measured as ppm Mauna Loa, 2017. Then an ice core was used with the aim of reconstructing the past decadal $CO_2$ values; these results have been obtained by Ahn et al., 2012 form the article "*Atmospheric CO2 over the last 1000 years: A high-resolution record from the West Antarctic Ice Sheet (WAIS) Divide ice core*" **(green curve)** where a decadal resolved record of atmospheric CO2 concentration has been reported for the last 1000 years, obtained from the West Antarctic Ice Sheet (WAIS) Divide shallow ice core. The results are statistically correlated with northern hemispheric climate and tropical Indo-Pacific sea surface temperature although the exact relationship between $CO_2$ and climate remains elusive. To unify both $CO_2$ concentrations, historical $CO_2$ record derived from a spline fit (75 year cutoff) of the Law Dome DSS, DE08, and DE08-2 ice cores were used **(blue curve)** Law dome, 2017. Thereby it has been possible to have a long $CO_2$ concentration record which will allow to compare with the obtained results and discuss its effects on the studied foraminiferal species, although the results coming from different sources and therefore will have small differences between them.

Focusing only on the graph, the records clearly show that atmospheric $CO_2$ has been increasing above preindustrial levels since year CE1850, sharing common trends of $CO_2$ change on centennial to multicentennial time scales.

#### 4.2.1.2 Sea Surface Temperature (SST)

The Sea surface temperature of the studied area has been reconstructed for the years 2013 to 1696 with alkenones by *Belen Martrat*, researcher of *Universitat de Barcelona*. This results are still unpublished. The results show periods of time where the temperature were quite stable, as in the case of years between 1719 to 1669 and 1879 to 1786. While the rest of the values have considerable variation. An increase on temperature from year 1904 to 1996 and from then a big drop until 2013 is the most remarkable of this graph.

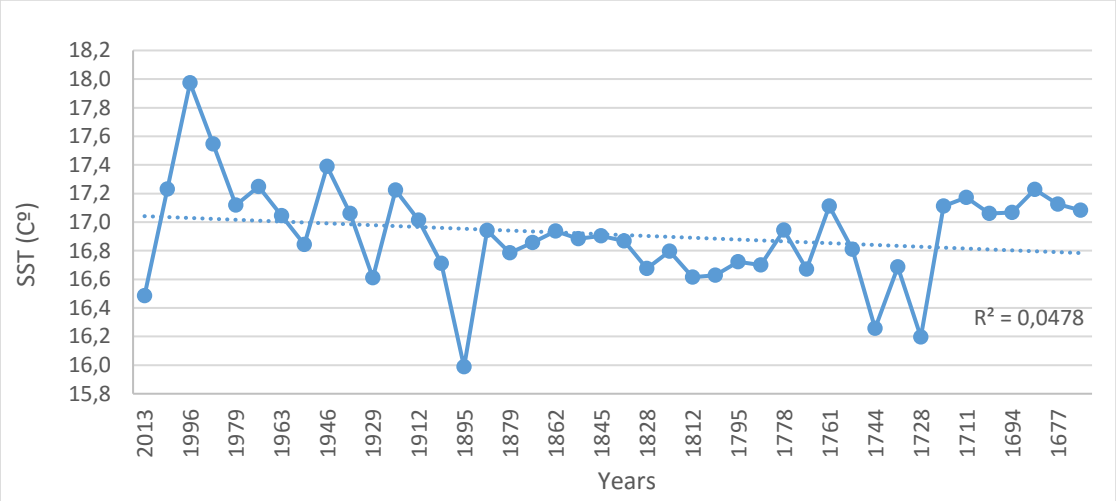


**Figure 25.** Annual Sea Surface temperature reconstruction with alkenones for the year 1669 to 2013 (Martrat, 2017).

#### 4.2.1.3 North Atlantic Oscillation (NAO)

Most of the Mediterranean region is indirectly under North Atlantic SST influence; this is one of the most important factors that drives the atmospheric circulation pattern of the northern hemisphere (Luterbacher, J., Xoplaki, 2003). Even on a longer time-scale, the Mediterranean region is linked to the North Atlantic through the North Atlantic Oscillation (NAO) variability, defined as the normalized winter difference in the sea-level pressure between the Azorean high and the Icelandic low cells (Hurrell, 1995). During the recent decades its major change at higher state has affected the whole Mediterranean Sea reducing westerlies precipitation that provides moisture and lowers the temperature in winter and increasing the penetration of the Azorean high pressure cell in summer causing more drought. In periods of positive NAO-index, westerlies blow over the western parts of northern Europe, while dry conditions are experienced in southern Europe and northern Africa. The situation is reversed during negative NAO-index periods (Incarbona et al., 2013).

Reconstruction of NOA monthly values from December 1658 to November 1900 and from December 1900 to December 2000, provided by Luterbacher et al., 2011 and Jr., 1980 respectively, become annual to be comparable with core 1 results:

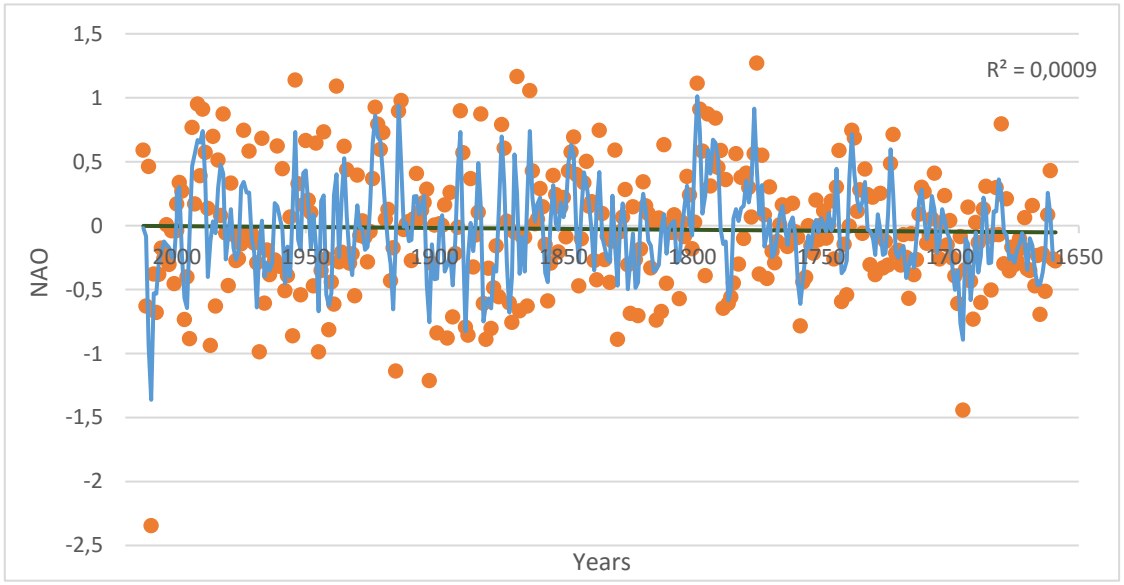


**Figure 27**. Annual North Atlantic Oscillation reconstruction from the years 1652 to 2000. The values from December 1658 to November 1900 are from Luterbacher et al., 2010 and from December 1900 to December 2000 by Jr., 1980.

As we could see on the graph, NOA values become more dispersed and variable over time. The tendency line shows that the results are slightly increasing.

#### 4.2.1.4 Historical Total Solar Irradiance

Historical Total Solar Irradiance (TSI) Reconstruction for the years 2009 to 1652 was computed by Greg Kopp, from the LASP Interactive Solar Irradiance Data (LISIRD) Center (ERDDAP, 2017). This data was obtained from (Wang, Lean, & Sheeley, Jr., 2005) and (Rottman, Woods, & George, 2005) with an offset -4.8178 W/m^2 to match SORCE/TIM absolute value. Extended using SORCE/TIM annual averages from 2003 onward.

This results indicate that the Total Solar Irradiance is becoming greater over time as the increasing tendency line shows.

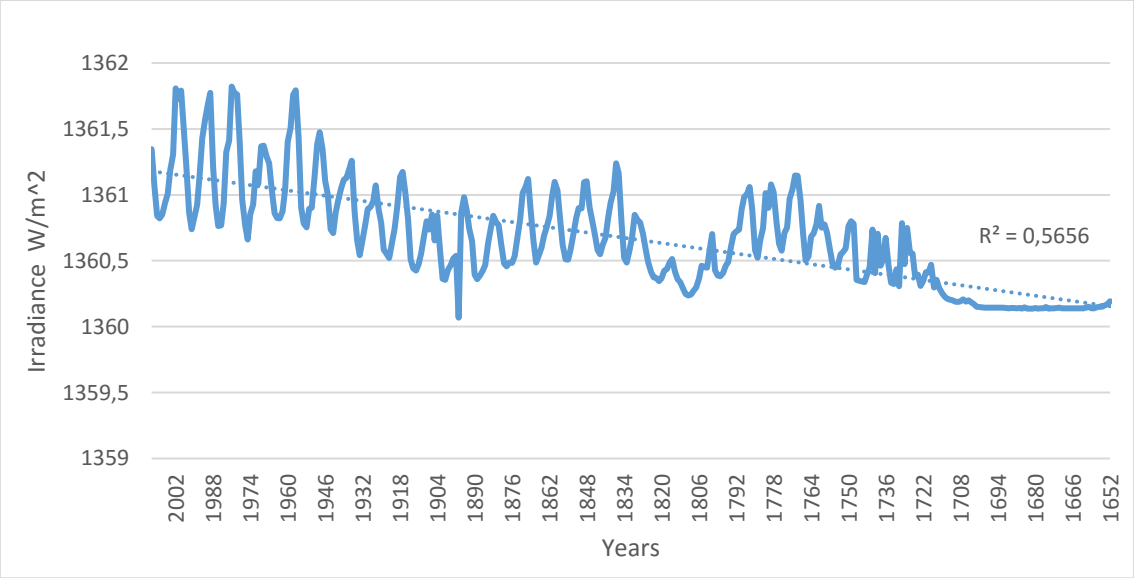


**Figure 28.** Historical Total Solar Irradiance (TSI) Reconstruction for the years 2009 to 1652 (ERDDAP, 2017).

### 4.2.2 Pearson correlation coefficients

Pearson's linear correlation coefficient (r) and the determination coefficient (p) were calculated in relation to the previous physical factors in order to explain the behaviour of the core 1 obtained data.

| $CO_2$ | Absolute abundance | | Relative abundance | | SNW | |
|---|---|---|---|---|---|---|
| *G. ruber* ss | -0,110 | 0,012 | 0,010 | 0,000 | 0,204 | 0,042 |
| *G. ruber* sl | -0,624 | 0,389 | -0,563 | 0,317 | -0,604 | 0,365 |
| *G. bulloides* | -0,301 | 0,091 | -0,170 | 0,029 | -0,209 | 0,044 |
| *G. inflata* | 0,009 | 0,000 | 0,505 | 0,255 | 0,104 | 0,011 |
| *G. truncatulinoides* | 0,171 | 0,029 | 0,450 | 0,202 | 0,376 | 0,141 |
| *O. universa* | 0,227 | 0,051 | 0,358 | 0,128 | | |
| *G. ruber* pink | -0,056 | 0,003 | 0,032 | 0,001 | | |
| Others | -0,609 | 0,370 | -0,548 | 0,300 | | |

| SST | Absolute abundance | | Relative abundance | | SNW | |
|---|---|---|---|---|---|---|
| *G. ruber* ss | -0,134 | 0,018 | -0,055 | 0,003 | -0,119 | 0,014 |
| *G. ruber* sl | -0,229 | 0,052 | -0,150 | 0,022 | -0,277 | 0,077 |
| *G. bulloides* | -0,088 | 0,008 | 0,184 | 0,034 | -0,269 | 0,072 |
| *G. inflata* | -0,218 | 0,047 | 0,051 | 0,003 | 0,273 | 0,075 |
| *G. truncatulinoides* | -0,051 | 0,003 | -0,044 | 0,002 | -0,268 | 0,072 |
| *O. universa* | 0,180 | 0,033 | 0,279 | 0,078 | | |
| *G. ruber* pink | -0,069 | 0,005 | 0,022 | 0,000 | | |
| Others | -0,226 | 0,051 | -0,176 | 0,031 | | |

| NAO | Absolute abundance | | Relative abundance | | SNW | |
|---|---|---|---|---|---|---|
| *G. ruber* ss | -0,075 | 0,006 | 0,065 | 0,004 | 0,057 | 0,003 |
| *G. ruber* sl | -0,107 | 0,012 | -0,111 | 0,012 | -0,221 | 0,049 |
| *G. bulloides* | -0,062 | 0,004 | 0,053 | 0,003 | -0,080 | 0,006 |
| *G. inflata* | -0,153 | 0,023 | 0,059 | 0,003 | 0,113 | 0,013 |
| *G. truncatulinoides* | -0,046 | 0,002 | -0,035 | 0,001 | 0,424 | 0,180 |
| *O. universa* | 0,178 | 0,032 | 0,207 | 0,043 | | |
| *G. ruber* pink | -0,197 | 0,039 | -0,167 | 0,028 | | |
| Others | -0,098 | 0,010 | -0,041 | 0,002 | | |

| TSI | Absolute abundance | | Relative abundance | | SNW | |
|---|---|---|---|---|---|---|
| *G. ruber* ss | -0,036 | 0,001 | -0,034 | 0,001 | 0,418 | 0,175 |
| *G. ruber* sl | -0,412 | 0,170 | -0,507 | 0,257 | -0,518 | 0,268 |
| *G. bulloides* | 0,206 | 0,042 | 0,170 | 0,029 | 0,155 | 0,024 |
| *G. inflata* | 0,191 | 0,037 | 0,330 | 0,109 | 0,026 | 0,001 |
| *G. truncatulinoides* | 0,354 | 0,126 | 0,206 | 0,043 | 0,589 | 0,347 |
| *O. universa* | 0,129 | 0,017 | 0,131 | 0,017 | | |
| *G. ruber* pink | -0,063 | 0,004 | -0,055 | 0,003 | | |
| Others | -0,247 | 0,061 | -0,434 | 0,188 | | |

**Table 8.** Pearson's linear correlation coefficient (left) and the determination coefficient (right) for the values obtained related to physical factors. p = 0.04 means low correlation, 0.05 < p > 0.1 means notable correlation and p < 0.1 means high correlation.

### 4.2.3 Analysis of the possible environmental factors loadings to the obtained results

#### 4.2.3.1 *Globigerinoides ruber*

*G. ruber* sensu stricto is the shallowest of the picked species, generally inhabits the upper 30 m of the water column, calcifies at relative warmer temperatures, and is one of the most tolerant species to low Sea Surface Salinity (SSS) and presents symbiosis with dinoflagellates.

The results of Pearson correlation coefficient about the different physical factors analysed show a high determination coefficient for the relation between SNW and Total Solar Irradiation. A coefficient of a 41.8% indicates a positive correlation of both parameters, which explains why the growth of its SNW due to TSI had increased over the years. *G. ruber* sensu stricto SNW also show a low relation with $CO_2$ of a 20.4% affirming that higher $CO_2$ atmospheric penetration to the ocean will increase its calcification. According to the results photosynthesis stimulates calcification, a stimulation of photosynthesis (which removes $CO_2$ and increases $CO_3^{2-}$) by ocean acidification could benefit calcification by mitigating the limited supply of carbonate ions. This may be due to the symbiotic relationship that they maintain with the dinoflagellates, where an increase of $CO_2$ and irradiance benefits photosynthesis, generating an increase in productivity.

*G. ruber* sensu lato is together with *G. ruber* sensu stricto the most tolerant species to low Sea Surface Salinity (SSS) and has symbiosis with dinoflagellates. Conversely *G. ruber* sensu lato calcifies at cooler temperatures than *G. ruber* sensu stricto and deeper depths up to 50 m.

The relevant decrease of its both abundances and SNW is strongly related with TSI but especially to $CO_2$. Both physical parameters show a negative Pearson correlation coefficient, conversely to *G. ruber* sensu stricto, confirming that *G. ruber* sensu lato calcification stimulates photosynthesis. A decrease in calcification generated by ocean acidification had a negative effect on photosynthesis, which explains the decrease of its parameters while $CO_2$ ant TSI have been increasing over the years. *G. ruber* sensu lato absolute abundance and SNW have a notable relation with SST, where the increase on SST is one of the contributors of the decrease on absolute abundance and SNW. The SST increase from year 1904 to 1996 and the posterior drop until 2013 explains the fall of almost 24% on *G. ruber* sensu lato SNW from year CE 1963 until the last recorded year. *G. ruber* sensu lato SNW also has correlation with NAO with its low negative values recorded since 2000, while less dry conditions are experienced in southern Europe, allowing a slight increase in *G. ruber* sensu lato SNW.

*G. ruber* pink is considered a summer species because it prefers warmer habitats than *G. ruber* white (Bé, 1967), lives in depths down to 50 m, does not present symbiosis and is less tolerant to Sea Surface Salinity (SSS) changes than *G. ruber* sensu lato and *G. ruber* sensu stricto.

The low p-value between *G. ruber* pink absolute abundance to NAO explains the inverse correlation between *G. ruber* pink absolute abundance values with this physical factor. The non-existent correlation of *G. ruber* pink with the other studied factors implies that NAO increase is the only cause of *G. ruber* pink absolute abundance decrease. But taking into account *G. ruber* pink ecologic preferences of high salinity water masses, a decrease of salinity due to ocean acidification could be the main reason of its abundance decrease. Unfortunately salinity data was not possible to obtain to corroborate it.

#### 4.2.3.2 *G. bulloides*

*Globigerina bulloides* mainly dwells above the thermocline within the upper 60 m of the water column. Its ecologic preferences are cool and eutrophic waters, usually associated with temperate to sub-polar water masses.

$CO_2$ is the physical parameter that shows highest p-values respect to *G. bulloides* both abundances and SNW within a negative correlation of 62.4% in absolute abundance, 56.3% in relative abundance and 60.4% in SNW. Concluding that a notable increase of atmospheric $CO_2$ that penetrates later to the sea, is affecting considerably *G. bulloides* calcification and abundance, confirming its decreasing values in post-industrial percentage of variation. A notable inverse correlation between SST with *G. bulloides* SNW of 27.7% is also an important parameter to highlight with respect to *G. bulloides,* for which the increase on SST will continuing reducing its calcification. The highest and the lowest peaks of years 1996 and 1895 in the SST plot are the reason for the lowest and the highest peaks of years 1992 and 1908 in *G. bulloides* SNW post-industrial levels relating this years with nutrient upwelling due to the less stratification by the decrease of SST. *G. bulloides* absolute abundance also shows a low positive correlation with TSI, which means that the increase in solar irradiance allows the increase of *G. bulloides* absolute abundance, which counteracts its decrease by CO2 and SST.

#### 4.2.3.3 *G. inflata*

*G. inflata* shows relations with sea surface temperature, salinity, and temperature at 200 m but has broad tolerances for these parameters. It has preferences for water masses with little seasonal variation in salinity and shows close relations with winter conditions in the vertical temperature gradient, surface water density, and stratification.

The relative abundance of *G. inflata* presents high positive correlation with $CO_2$ and TSI, 50.5% and 33% respectively, assuming that the increase in both factors had also increased *G. inflata* relative abundance especially since post-industrial levels. SST also plays an important role in *G. inflate* more concretely with low negative correlation 19.7% on it absolute abundance and a notable positive correlation of 27.3% on its SNW, so the increasing values of SST are reducing *G. inflata* absolute abundance but conversely its calcification (SNW) increases, being less number of specimens but highly calcified. Consequently, an increase in SST benefits calcification. The fall of SST on year 1929 is also shown in *G. inflate* SNW plot on the same year.

#### 4.2.3.4 *G. truncatulinoides*

*Globorotalia truncatulinoides* populates the deepest habitat of all extant species, having been sampled alive from the water column below 2000 m water depth (Schiebel & Hemleben, 2005). It is typically a subtropical species that occurs over a broad range of salinities and sea surface temperatures. It prefers areas with little seasonality in salinity, in contrast to broad tolerances for seasonal change in sea surface temperatures.

*G. truncatulinoides* SNW presents a relationship with the four studied physical parameters. A negative correlation of a 26.8% is with SST meanwhile the rest, $CO_2$, NAO and TSI, have a positive correlation of 37.6%, 42.4% and 58.9% respectively. So *G. truncatulinoides* calcification has diminished due to an increase on SST but it is also favoured by the increase of $CO_2$, NAO and TSI. The highest peak on *G. truncatulinoides* SNW of year 1992 is related to one of NAO highest peaks in the same year. The strangest thing is that *G. truncatulinoides* and *G. bulloides* have almost equal Pearson correlation coefficients and the same inverse relation with the SST; their values of SNW are inverse between them. And the reason why post-industrial period *G. truncatulinoides* SNW has increased so steadily is due to $CO_2$, NAO and TSI.

Apart from that, *G. truncatulinoides* relative abundance presents a high positive correlation with $CO_2$ of 45%, and also a low positive correlation of a 20.6% with TSI, such that both increasing parameters have increased the relative abundance of the species. Also, a high positive correlation between TSI and *G. truncatulinoides* absolute abundance of a 35.4% indicates that the increase of solar irradiance allows the increase of its absolute abundance.

#### 4.2.3.5 *Orbulina universa*

*Orbulina universa* is one of the most widely distributed species among planktic foraminifera, whereby its relative abundance hardly ever exceeds 3-4 %. It tolerates wide ranges of ambient water salinity and temperature, is abundant from tropical to temperate waters (de Vargas et al., 1999) and has symbiosis with dinoflagellates.

Its relative abundance has a positive correlation from high to lower coefficient with $CO_2$, SST and NAO. The increase in the last 200 years of these parameters, especially $CO_2$, may allow the increase of a 25% on *O. universa* relative abundance with respect to the period of non-human alteration. $CO_2$ also has notably positive correlation with *O. universa* absolute abundance that will be the cause of its 1.08 ($g^{-1}$) increase difference between post and pre-industrial times.

#### 4.2.3.6 Others

The reduction in others absolute abundance is significantly and mostly affected by the increase of $CO_2$ but also for the increase of TSI and SST, due to these parameters having a negative correlation with others absolute abundance. A large peak in others absolute abundance at year 1753 is closely related to a decline of solar irradiance happening in that year.

The increase of $CO_2$ concentration and solar irradiance are the main causes of the decrease of 57.37% in others relative abundance. Both parameters have a negative high correlation with the relative abundance, but $CO_2$ is the more significant.

It is clearly observed how both abundances have diminished due to the increase of $CO_2$ concentration in the atmosphere. So it is safe to assume that the increase of $CO_2$ is the main cause of the decline on biodiversity.

# 5. Conclusions

The Mediterranean Sea is one of the most affected oceanic regions by acidification (Hassoun et al., 2015) for the following reasons: it is a semi-enclosed and shallower sea with higher evaporation rates, overturning circulation, high alkalinity and temperature throughout the water column that only surface anthropogenic $CO_2$ loaded waters are inflowing from the Atlantic to the Mediterranean Sea. The present exorbitant anthropogenic $CO_2$ concentrations just make this effect significantly aggravated. Ocean uptake of anthropogenic $CO_2$ increases the concentration of hydrogen ions, decreasing the sea water pH and producing ocean acidification. As a consequence of ocean acidification all biological and biogeochemical processes are direct and indirect potentially affected. Disturbances in the acid-base status of organisms, changes in calcification with the decline on the calcification rate, and also changes in photosynthesis are just a few examples of cascading effects that could occur at any ecological level.

The modification of the water column conditions due to the considerable increase of atmospheric $CO_2$ that penetrates to the superficial Sea waters, indicates changes in ecological conditions all over the studied period, but especially from approximately year CE 1840 until today. The large differences between species absolute abundance, relative abundance and SNW have been shown to be related whit disturbances to the following physical factors: sea surface temperature, salinity, stratification, pH and $CO_3^{-2}$ concentration.

From the results obtained in the studied area, an abundance decrease and calcification increase have happened during the study period from 2013 to 1652. Differences between post and pre industrial times are highly significant, meaning that humanity has altered and is still altering the climate system dynamics and consequently the ocean system.

$CO_2$ is the main cause of specimens abundance reduction while it is the second main cause of increase in foraminiferal calcification, being solar irradiance the main cause. The increase of SST reduces both abundance and calcification. So acidification in that case reduces foraminiferal abundance and increases its calcification, meanwhile warming is deteriorating foraminifera.

Humans have economic, cultural, societal, and nutritional dependency to the oceans but we are the disruptors of the earth system that have also potentially catastrophic consequences for the ocean carbonate system. These changes detected on the studied foraminiferal species are only an example of how acidification puts humanity in a vulnerable situation with the risks to economic and society welfare, and how this effect could happen on a higher scale including disturbances to seafood resources and the deterioration of coral reefs, decreasing the entire Mediterranean Sea richness and biodiversity.

# 6. Acknowledgements

Thanks for all the knowledge and support received from my supervisors Patrizia Ziveri and Graham Mortyn. To my colleagues Michael Grelaud and Giselda Anglada for holding and help me to solve all my doubts. And I would also to thank Patrizia for giving me the opportunity to work at ICTA, experience the research work at firsthand and discover the interesting field of paleoceanography. This unforgettable experience, of which I am very satisfied, has marked the course of my life and has allowed me to decide what I want to do in the nearly future.

# 7. Bibliography


Ahn, J., Brook, E. J., Mitchell, L., Rosen, J., McConnell, J. R., Taylor, K., … Rubino, M. (2012). Atmospheric CO2 over the last 1000 years: A high-resolution record from the West Antarctic Ice Sheet (WAIS) Divide ice core. *Global Biogeochemical Cycles*, *26*(2), 1–11. https://doi.org/10.1029/2011GB004247

Alley, R., Berntsen, T., Bindoff, N. L., Chen, Z., Chidthaisong, A., Friedlingstein, P., … Zwiers, F. (2007). INTERGOVERNMENTAL PANEL ON CLIMATE CHANGE Climate Change 2007: The Physical Science Basis Summary for Policymakers Contribution of Working Group I to the Fourth Assessment Report of the Intergovernmental Panel on Climate Change. Retrieved from http://www.ipcc.ch

Álvarez, M. (Marta). (2011). The CO2 system observations in the Mediterranean Sea: past, present and future, in: CIESM monograph 43: Designing Med-SHIP: a program for repeated oceanographic surveys. Retrieved from http://agris.fao.org/agris-search/search.do?recordID=ES2015B01736

André, A., Quillévéré, F., Morard, R., Ujiié, Y., Escarguel, G., de Vargas, C., … Douady, C. J. (2014). SSU rDNA Divergence in Planktonic Foraminifera: Molecular Taxonomy and Biogeographic Implications. *PLoS ONE*, *9*(8), e104641. https://doi.org/10.1371/journal.pone.0104641

Anglada, G. (2016). *Planktic foraminiferal species and mass dynamics during the last few centuries: A case study in the North-Western Mediterranean Sea (Unpublished Master's Thesis)*. UB / UAB, Catalunya.

Aurahs, R., Göker, M., Grimm, G. W., Hemleben, V., Hemleben, C., Schiebel, R., & Kucera, M. (2009). Using the Multiple Analysis Approach to Reconstruct Phylogenetic Relationships among Planktonic Foraminifera from Highly Divergent and Length-polymorphic SSU rDNA Sequences. *Bioinformatics and Biology Insights*, *3*, 155–77. Retrieved from http://www.ncbi.nlm.nih.gov/pubmed/20140067

Aurahs, R., Treis, Y., Darling, K., & Kucera, M. (2011). A revised taxonomic and phylogenetic concept for the planktonic foraminifer species Globigerinoides ruber based on molecular and morphometric evidence. *Marine Micropaleontology*, *79*(1–2), 1–14. https://doi.org/10.1016/j.marmicro.2010.12.001

Bauska, T. K., Joos, F., Mix, A. C., Roth, R., Ahn, J., & Brook, E. J. (2015). Links between atmospheric carbon dioxide, the land carbon reservoir and climate over the past millennium. *NATURE GEOSCIENCE Www.nature.com*, *8*. https://doi.org/10.1038/NGEO2422

Be, A. W. H., Harrison, S. M., & Lott, L. (1973). Orbulina universa d'Orbigny in the Indian Ocean. *Micropaleontology*, *19*(2). Retrieved from http://micropal.geoscienceworld.org/content/19/2/150

Bé, A. W. H., Hutson, W. H., & Be, A. W. H. (1977). Ecology of Planktonic Foraminifera and Biogeographic Patterns of Life and Fossil Assemblages in the Indian Ocean. *Micropaleontology*, *23*(4), 369. https://doi.org/10.2307/1485406

Béranger, K., Mortier, L., & Crépon, M. (2005). Seasonal variability of water transport through the Straits of Gibraltar, Sicily and Corsica, derived from a high-resolution model of the Mediterranean circulation. *Progress in Oceanography*, *66*(2–4), 341–364.

https://doi.org/10.1016/j.pocean.2004.07.013

Brown, E. A., Flower, B. P., & Williams, C. (2012). Evaluation of Two Globigerinoides ruber (white) Morphotypes in Paleoceanographic Reconstruction: A Gulf of Mexico Case Study. *American Geophysical Union, Fall Meeting 2012, Abstract #PP43A-2010*. Retrieved from http://adsabs.harvard.edu/abs/2012AGUFMPP43A2010B

de Vargas, C., Norris, R., Zaninetti, L., Gibb, S. W., & Pawlowski, J. (1999). Molecular evidence of cryptic speciation in planktonic foraminifers and their relation to oceanic provinces. *Proceedings of the National Academy of Sciences of the United States of America*, *96*(6), 2864–8. https://doi.org/10.1073/PNAS.96.6.2864

Egleston, E. S., Sabine, C. L., & Morel, F. M. M. (2010). Revelle revisited: Buffer factors that quantify the response of ocean chemistry to changes in DIC and alkalinity. *Global Biogeochemical Cycles*, *24*(1), n/a-n/a. https://doi.org/10.1029/2008GB003407

ERDDAP. (2017). Historical Total Solar Irradiance Reconstruction. Retrieved August 27, 2017, from http://coastwatch.pfeg.noaa.gov/erddap/tabledap/earthCubeLisirdHistTsi.graph

Garcia, C. O. (2011). *Evaluating the reliability of 210 Pb-dated peat bog cores to reconstruct atmospheric metal deposition in NW Spain*. UAB, Catalunya.

Garrett, C. (1994). The Mediterranean Sea as a Climate Test Basin. In *Ocean Processes in Climate Dynamics: Global and Mediterranean Examples* (pp. 227–237). Dordrecht: Springer Netherlands. https://doi.org/10.1007/978-94-011-0870-6_10

Gattuso, J.-P., & Hansson, L. (2011). *Ocean acidification*. Oxford University Press. Retrieved from https://books.google.es/books?hl=ca&lr=&id=eoxpAgAAQBAJ&oi=fnd&pg=PA1&dq=ocean+acidification+&ots=0WwIstRgn3&sig=Yj_PtL9gqhBTYOCVKc7T6i7bSQ8#v=onepage&q=ocean acidification&f=false

Gattuso, J.-P., & Lavigne, H. (2009). Technical Note: Approaches and software tools to investigate the impact of ocean acidification. *Biogeosciences*, *6*, 2121–2133. Retrieved from www.biogeosciences.net/6/2121/2009/

Hassoun, A. E. R., Gemayel, E., Krasakopoulou, E., Goyet, C., Abboud-Abi Saab, M., Guglielmi, V., … Falco, C. (2015). Acidification of the Mediterranean Sea from anthropogenic carbon penetration. *Deep Sea Research Part I: Oceanographic Research Papers*, *102*, 1–15. https://doi.org/10.1016/j.dsr.2015.04.005

Hemleben, C., Spindler, M., Breitinger, I., & Deuser, W. G. (1985). Field and laboratory studies on the ontogeny and ecology of some globorotaliid species from the Sargasso Sea off Bermuda. *Journal of Foraminiferal Research*, *15*(4). Retrieved from http://jfr.geoscienceworld.org/content/15/4/254

Hurrell, J. W. (1995). Decadal Trends in the North Atlantic Oscillation: Regional Temperatures and Precipitation. *Science*, *Vol. 269,* 676–679. https://doi.org/10.2307/2888966

Incarbona, A., Sprovieri, M., Di Stefano, A., Di Stefano, E., Salvagio Manta, D., Pelosi, N., … Ziveri, P. (2013). Productivity modes in the mediterranean sea during dansgaard-oeschger (20,000-70,000yr ago) oscillations. *Palaeogeography, Palaeoclimatology, Palaeoecology*, *392*, 128–137. https://doi.org/10.1016/j.palaeo.2013.09.023

Jr., K. E. T. and D. A. P. (1980). The Northern Hemisphere Sea-Level Pressure Data Set: Trends, Errors and Discontinuities. *Online Journal AMS*. https://doi.org/https://doi.org/10.1175/1520-0493(1980)108<0855:TNHSLP>2.0.CO;2

Krishnaswamy, S., Lal, D., Martin, J. M., & Meybeck, M. (1971). Geochronology of lake sediments. *Earth and Planetary Science Letters*, *11*(1–5), 407–414. https://doi.org/10.1016/0012-821X(71)90202-0

Law dome. (2017). Historical CO2 record derived from a spline fit (75 year cutoff) of the Law Dome DSS, DE08, and DE08-2 ice cores. Retrieved from http://cdiac.ornl.gov/ftp/trends/co2/lawdome.smoothed.yr75

Lončarić, N., van Iperen, J., Kroon, D., & Brummer, G.-J. A. (2007). Seasonal export and sediment preservation of diatomaceous, foraminiferal and organic matter mass fluxes in a trophic gradient across the SE Atlantic. *Progress in Oceanography*, *73*(1), 27–59. https://doi.org/10.1016/j.pocean.2006.10.008

Luterbacher, J., Xoplaki, E. (2003). 500-yearWinter temperature and precipitation variability over the Mediterranean area and its connection to the large-scale atmospheric circulation. *Bolle, H.J. (Ed.), Mediterranean Climate, Variability and Trends.*, *Springer-V*, 133–154. https://doi.org/http://dx.doi.org/10.1016/j.palaeo.2013.09.023

Luterbacher, J., Xoplaki, E., Dietrich, D., Jones, P. D., Davies, T. D., Portis, D., … Wanner, H. (2011). Extending North Atlantic oscillation reconstructions back to 1500. *Atmospheric Science Letters*, *Volume 2*(Issue 1-4), Pages 114–124. https://doi.org/10.1006/asle.2002.0047

Martrat, B. (2017). *Core 1 SST reconstruction by alkenones. (Unpublished work)*. Barcelona.

Mauna Loa. (2017). No Title. Retrieved August 12, 2017, from ftp://aftp.cmdl.noaa.gov/products/trends/co2/co2_annmean_mlo.txt

Millot, C. (2009). Another description of the Mediterranean Sea outflow. *Progress in Oceanography*, *82*(2), 101–124. https://doi.org/10.1016/j.pocean.2009.04.016

Morard, R., Quillévéré, F., Douady, C. J., de Vargas, C., de Garidel-Thoron, T., & Escarguel, G. (2011). Worldwide Genotyping in the Planktonic Foraminifer Globoconella inflata: Implications for Life History and Paleoceanography. *PLoS ONE*, *6*(10), e26665. https://doi.org/10.1371/journal.pone.0026665

Movellan, A., Schiebel, R., Zubkov, M. V, Smyth, A., & Howa, H. (2012). Protein biomass quantification of unbroken individual foraminifers using nano-spectrophotometry. *Biogeosciences*, *9*, 3613–3623. https://doi.org/10.5194/bg-9-3613-2012

NOAA. (2017a). Globigerina bulloides d'Orbigny, 1826. Retrieved from https://www.ngdc.noaa.gov/mgg/geology/hh1996/bulloides.html

NOAA. (2017b). Globorotalia inflata (d'Orbigny, 1839). Retrieved from https://www.ngdc.noaa.gov/mgg/geology/hh1996/inflata.html

NOAA. (2017c). Globorotalia truncatulinoides (d'Orbigny, 1839). Retrieved from https://www.ngdc.noaa.gov/mgg/geology/hh1996/trunc.html

NOAA. (2017d). Orbulina universa d'Orbigny, 1839. Retrieved from https://www.ngdc.noaa.gov/mgg/geology/hh1996/universa.html

Onken, R., Álvarez, A., Fernández, V., Vizoso, G., Basterretxea, G., Tintoré, J., … Nacini, E. (2008). A forecast experiment in the Balearic Sea. *Journal of Marine Systems*, *71*(1–2), 79–98. https://doi.org/10.1016/j.jmarsys.2007.05.008

Pak, D. K., Clayman, L., Weaver, J., Schimmelmann, A., & Hendy, I. L. (2011). Planktonic foraminiferal shell weight reflects sea surface temperature over the past 150 years in Santa Barbara Basin, California. *American Geophysical Union, Fall Meeting 2011, Abstract #PP41C-1787*. Retrieved from http://adsabs.harvard.edu/abs/2011AGUFMPP41C1787P

Rohling, E. ., Sprovieri, M., Cane, T., Casford, J. S. ., Cooke, S., Bouloubassi, I., … Kroon, D. (2004). Reconstructing past planktic foraminiferal habitats using stable isotope data: a case history for Mediterranean sapropel S5. *Marine Micropaleontology*, *50*(1–2), 89–123.

https://doi.org/10.1016/S0377-8398(03)00068-9

Rohling, E. J., Marino, G., & Grant, K. M. (2015). Mediterranean climate and oceanography, and the periodic development of anoxic events (sapropels). *Earth-Science Reviews*, *143*, 62–97. https://doi.org/10.1016/j.earscirev.2015.01.008

Rottman, G., Woods, T., & George, V. (Eds.). (2005). *The Solar Radiation and Climate Experiment (SORCE)*. New York, NY: Springer New York. https://doi.org/10.1007/0-387-37625-9

Sabine, C. L., & Tanhua, T. (2010). Estimation of Anthropogenic CO 2 Inventories in the Ocean. *Annual Review of Marine Science*, *2*(1), 175–198. https://doi.org/10.1146/annurev-marine-120308-080947

Sanchez-Cabeza, J. A., Masqué, P., & Ani-Ragolta, I. (1998). 210Pb and210Po analysis in sediments and soils by microwave acid digestion. *Journal of Radioanalytical and Nuclear Chemistry*, *227*(1–2), 19–22. https://doi.org/10.1007/BF02386425

Schellnhuber, H. J., Cramer, W., Nakicenovic, N., Wigley, T., & Yohe, G. (2006). Avoiding Dangerous Climate Change Editor in Chief Co-editors. Retrieved from www.cambridge.org

Schiebel, R., & Hemleben, C. (2005). Modern planktic foraminifera. *Paläontologische Zeitschrift*, *79*(1), 135–148. https://doi.org/10.1007/BF03021758

Schiebel, R., & Hemleben, C. (2017). *Planktic Foraminifers in the Modern Ocean*. https://doi.org/10.1007/978-3-662-50297-6

Schneider, C. A., Rasband, W. S., and Eliceiri, K. W. (2012). NIH Image to ImageJ: 25 years of image analysis. *Nat. Methods*, *9*(Historical Commentary), 671–675. https://doi.org/doi:10.1038/nmeth.2089

Spero, H. J. (1988). Ultrastructural examination of chamber morphogenesis and biomineralization in the planktonic foraminiferOrbulina universa. *Marine Biology*, *99*(1), 9–20. https://doi.org/10.1007/BF00644972

Stratford, K., & Williams, R. G. (1997). A tracer study of the formation, dispersal, and renewal of Levantine Intermediate Water. *Journal of Geophysical Research: Oceans*, *102*(C6), 12539–12549. https://doi.org/10.1029/97JC00019

Stratford, K., Williams, R. G., & Drakopoulos, P. G. (1998). Estimating climatological age from a model-derived oxygen–age relationship in the Mediterranean. *Journal of Marine Systems*, *18*(1–3), 215–226. https://doi.org/10.1016/S0924-7963(98)00013-X

Thorpe, S. A. (Oceanographer). (2009). Encyclopedia of ocean sciences : ocean currents, 647. Retrieved from https://books.google.es/books?hl=es&lr=&id=FYSCUH235E8C&oi=fnd&pg=PA283&dq=mediterranean+sea+circulation&ots=1S2aHEpy9o&sig=9Jg5pSmcIf8ETQINPrqjNuc8Mz4#v=onepage&q=mediterranean sea circulation&f=false

Touratier, F., & Goyet, C. (2009). Decadal evolution of anthropogenic CO2 in the northwestern Mediterranean Sea from the mid-1990s to the mid-2000s. *Deep Sea Research Part I: Oceanographic Research Papers*, *56*(10), 1708–1716. https://doi.org/10.1016/j.dsr.2009.05.015

US Department of Commerce, NOAA, E. S. R. L. (2017). ESRL Global Monitoring Division - Global Greenhouse Gas Reference Network. Retrieved from https://www.esrl.noaa.gov/gmd/ccgg/trends/full.html

Wang, Y. -M., Lean, J. L., & Sheeley, Jr., N. R. (2005). Modeling the Sun's Magnetic Field and Irradiance since 1713. *The Astrophysical Journal*, *625*(1), 522–538. https://doi.org/10.1086/429689

WEINER, A., AURAHS, R., KURASAWA, A., KITAZATO, H., & KUCERA, M. (2012). Vertical niche partitioning between cryptic sibling species of a cosmopolitan marine planktonic protist. *Molecular Ecology*, *21*(16), 4063–4073. https://doi.org/10.1111/j.1365-294X.2012.05686.x

Wüst, G. (1961). On the vertical circulation of the Mediterranean Sea. *Journal of Geophysical Research*, *66*(10), 3261–3271. https://doi.org/10.1029/JZ066i010p03261

Zeebe, R. E. (2012). History of Seawater Carbonate Chemistry, Atmospheric CO $_2$ , and Ocean Acidification. *Annual Review of Earth and Planetary Sciences*, *40*(1), 141–165. https://doi.org/10.1146/annurev-earth-042711-105521

Zeebe, R. E., & Wolf-Gladrow, D. A. (n.d.). *CO2 in seawater : equilibrium, kinetics, isotopes*. Retrieved from https://books.google.es/books?hl=es&lr=&id=g3j3Zn4kEscC&oi=fnd&pg=PA1&dq=Zeebe+and+Wolf-Gladrow+2001&ots=lbQtL4ueqO&sig=lbiUKacK5oAfq38-7oGELsGCJaM#v=onepage&q=Zeebe and Wolf-Gladrow 2001&f=false

# 8. Appendix

| Age model | depth | Age model | depth | Age model | depth | Age model | depth |
|---|---|---|---|---|---|---|---|
| *2013* | 0-0,5 | *1921* | 11-11,5 | *1828* | 22-22,5 | *1736* | 33-33,5 |
| *2009* | 0,5-1 | *1916* | 11,5-12 | *1824* | 22,5-23 | *1732* | 33,5-34 |
| *2005* | 1-1,5 | *1912* | 12-12,5 | *1820* | 23-23,5 | *1728* | 34-34,5 |
| *2000* | 1,5-2 | *1908* | 12,5-13 | *1816* | 23,5-24 | *1723* | 34,5-35 |
| *1996* | 2-2,5 | *1904* | 13-13,5 | *1812* | 24-24,5 | *1719* | 35-35,5 |
| *1992* | 2,5-3 | *1900* | 13,5-14 | *1807* | 24,5-25 | *1715* | 35,5-36 |
| *1988* | 3-3,5 | *1895* | 14-14,5 | *1803* | 25-25,5 | *1711* | 36-36,5 |
| *1984* | 3,5-4 | *1891* | 14,5-15 | *1799* | 25,5-26 | *1707* | 36,5-37 |
| *1979* | 4-4,5 | *1887* | 15-15,5 | *1795* | 26-26,5 | *1702* | 37-37,5 |
| *1975* | 4,5-5 | *1883* | 15,5-16 | *1791* | 26,5-27 | *1698* | 37,5-38 |
| *1971* | 5-5,5 | *1879* | 16-16,5 | *1786* | 27-27,5 | *1694* | 38-38,5 |
| *1967* | 5,5-6 | *1874* | 16,5-17 | *1782* | 27,5-28 | *1690* | 38,5-39 |
| *1963* | 6-6,5 | *1870* | 17-17,5 | *1778* | 28-28,5 | *1686* | 39-39,5 |
| *1958* | 6,5-7 | *1866* | 17,5-18 | *1774* | 28,5-29 | *1681* | 39,5-40 |
| *1954* | 7-7,5 | *1862* | 18-18,5 | *1770* | 29-29,5 | *1677* | 40-40,5 |
| *1950* | 7,5-8 | *1855* | 18,5-19 | *1765* | 29,5-30 | *1673* | 40,5-41 |
| *1946* | 8-8,5 | *1853* | 19-19,5 | *1761* | 30-30,5 | *1669* | 41-41,5 |
| *1942* | 8,5-9 | *1849* | 19,5-20 | *1757* | 30,5-31 | *1665* | 41,5-42 |
| *1937* | 9-9,5 | *1845* | 20-20,5 | *1753* | 31-31,5 | *1660* | 42-42,5 |
| *1933* | 9,5-10 | *1841* | 20,5-21 | *1749* | 31,5-32 | *1656* | 42,5-43 |
| *1929* | 10-10,5 | *1837* | 21-21,5 | *1744* | 32-32,5 | *1652* | 43-43,5 |
| *1925* | 10,5-11 | *1832* | 21,5-22 | *1740* | 32,5-33 | | |

**Table 9.** Years corresponding to de centimetres depth as referred by the edge model.

| Year | *G. ruber* ss | *G. ruber* sl | *G. bulloides* | *G. inflata* | *G. truncatulinoides* | *O. universa* | *G. ruber pink* | Others | TOTAL |
|---|---|---|---|---|---|---|---|---|---|
| *2013* | 0,446 | 0,074 | 5,052 | 3,418 | 4,086 | 0,000 | 0,000 | 1,263 | 13,893 |
| *2009* | 0,346 | 0,346 | 5,882 | 4,671 | 5,190 | 0,692 | 0,346 | 1,557 | 18,685 |
| *2005* | 0,260 | 0,433 | 6,759 | 2,426 | 3,293 | 0,260 | 0,260 | 1,127 | 14,558 |
| *2000* | 0,117 | 0,702 | 6,667 | 3,041 | 4,444 | 0,234 | 0,234 | 1,287 | 16,608 |
| *1996* | 0,235 | 1,056 | 8,568 | 4,577 | 3,756 | 0,469 | 0,000 | 0,822 | 19,249 |
| *1992* | 0,179 | 0,538 | 5,197 | 4,480 | 3,226 | 0,538 | 0,000 | 1,434 | 15,412 |
| *1988* | 0,275 | 0,412 | 5,769 | 5,220 | 2,610 | 0,000 | 0,412 | 1,648 | 16,071 |
| *1984* | 0,142 | 0,426 | 5,824 | 4,119 | 2,699 | 0,426 | 0,000 | 1,136 | 14,631 |
| *1979* | 0,581 | 0,145 | 8,430 | 4,506 | 2,616 | 0,291 | 0,145 | 1,744 | 17,878 |
| *1975* | 0,000 | 0,179 | 8,057 | 5,192 | 4,118 | 0,269 | 0,090 | 1,701 | 19,606 |
| *1971* | 0,155 | 0,465 | 11,318 | 8,217 | 6,667 | 0,000 | 0,000 | 2,171 | 28,837 |
| *1967* | 0,179 | 0,536 | 8,132 | 3,753 | 4,647 | 0,715 | 0,179 | 1,519 | 19,482 |
| *1963* | 0,166 | 1,165 | 8,819 | 5,158 | 6,489 | 0,000 | 0,166 | 2,329 | 24,126 |
| *1958* | 0,125 | 0,878 | 15,056 | 4,141 | 6,524 | 0,376 | 0,000 | 2,886 | 29,862 |
| *1954* | 0,064 | 0,450 | 10,746 | 4,891 | 4,247 | 0,515 | 0,000 | 1,609 | 22,458 |
| *1950* | 0,260 | 0,911 | 16,667 | 5,078 | 4,297 | 0,260 | 0,000 | 2,344 | 29,557 |
| *1946* | 0,111 | 0,443 | 15,299 | 1,663 | 5,876 | 0,111 | 0,111 | 2,106 | 25,610 |
| *1942* | 0,344 | 1,376 | 15,138 | 4,358 | 6,193 | 0,000 | 0,573 | 2,752 | 30,390 |
| *1937* | 0,100 | 0,802 | 13,039 | 4,413 | 6,219 | 0,201 | 0,301 | 2,407 | 27,382 |
| *1933* | 0,347 | 1,733 | 13,172 | 4,333 | 6,412 | 0,347 | 0,000 | 2,426 | 28,423 |
| *1929* | 0,126 | 0,758 | 13,258 | 5,808 | 3,914 | 0,126 | 0,505 | 2,273 | 26,641 |
| *1925* | 0,284 | 0,782 | 8,955 | 3,625 | 3,483 | 0,498 | 0,426 | 1,777 | 19,545 |

| | | | | | | | | | |
|---|---|---|---|---|---|---|---|---|---|
| *1921* | 0,147 | 1,026 | 12,381 | 3,810 | 6,520 | 0,220 | 0,147 | 2,564 | 26,667 |
| *1916* | 0,537 | 1,252 | 17,174 | 3,399 | 4,114 | 0,358 | 0,179 | 2,683 | 29,159 |
| *1912* | 0,149 | 1,937 | 17,139 | 4,322 | 6,408 | 0,298 | 0,149 | 3,130 | 33,383 |
| *1908* | 0,701 | 0,100 | 14,815 | 4,505 | 5,405 | 0,300 | 0,100 | 2,703 | 27,928 |
| *1904* | 0,000 | 0,705 | 12,185 | 6,848 | 5,035 | 0,302 | 0,201 | 2,316 | 27,593 |
| *1900* | 0,225 | 1,050 | 16,054 | 5,026 | 4,651 | 0,225 | 0,075 | 2,851 | 29,932 |
| *1895* | 0,165 | 1,318 | 14,333 | 6,919 | 6,260 | 0,165 | 0,329 | 3,130 | 32,455 |
| *1891* | 0,265 | 0,927 | 13,775 | 7,285 | 5,033 | 0,132 | 0,000 | 2,914 | 30,066 |
| *1887* | 0,252 | 0,883 | 12,736 | 4,918 | 5,422 | 0,126 | 0,126 | 2,522 | 26,734 |
| *1883* | 0,423 | 0,564 | 11,566 | 5,360 | 6,065 | 0,141 | 0,000 | 2,257 | 25,952 |
| *1879* | 0,399 | 0,897 | 9,372 | 6,181 | 4,586 | 0,199 | 0,299 | 2,393 | 23,928 |
| *1874* | 0,506 | 1,180 | 12,648 | 6,745 | 8,094 | 0,253 | 0,000 | 3,035 | 31,956 |
| *1870* | 0,354 | 0,707 | 11,848 | 7,073 | 7,162 | 0,177 | 0,177 | 2,653 | 29,797 |
| *1866* | 0,474 | 2,017 | 14,947 | 6,762 | 3,796 | 0,356 | 0,119 | 2,966 | 30,961 |
| *1862* | 0,334 | 1,336 | 15,367 | 8,018 | 6,013 | 0,445 | 0,111 | 3,229 | 34,521 |
| *1855* | 0,399 | 1,065 | 10,786 | 9,188 | 5,459 | 0,133 | 0,133 | 2,530 | 29,294 |
| *1853* | 0,327 | 0,981 | 14,800 | 7,032 | 7,114 | 0,409 | 0,164 | 2,944 | 33,442 |
| *1849* | 0,153 | 0,612 | 11,009 | 5,810 | 5,352 | 0,000 | 0,153 | 2,599 | 25,535 |
| *1845* | 0,446 | 2,141 | 8,921 | 2,498 | 5,888 | 0,268 | 0,268 | 3,033 | 23,461 |
| *1841* | 0,595 | 2,378 | 7,253 | 4,281 | 4,994 | 0,119 | 0,000 | 1,665 | 21,284 |
| *1837* | 0,615 | 2,664 | 9,221 | 4,918 | 6,967 | 0,205 | 0,000 | 2,459 | 27,049 |
| *1832* | 0,452 | 1,582 | 10,508 | 5,085 | 5,424 | 0,226 | 0,113 | 3,729 | 27,119 |
| *1828* | 0,402 | 3,481 | 8,434 | 5,221 | 2,410 | 0,268 | 0,000 | 1,740 | 21,954 |
| *1824* | 0,487 | 1,825 | 9,124 | 4,136 | 4,745 | 0,122 | 0,122 | 2,190 | 22,749 |
| *1820* | 0,721 | 2,404 | 9,736 | 3,486 | 4,207 | 0,240 | 0,120 | 3,005 | 23,918 |
| *1816* | 0,602 | 2,857 | 9,023 | 3,459 | 3,459 | 0,301 | 0,000 | 2,406 | 22,105 |
| *1812* | 0,122 | 2,448 | 9,302 | 6,732 | 2,938 | 0,122 | 0,000 | 1,591 | 23,256 |
| *1807* | 0,467 | 2,570 | 8,645 | 3,855 | 2,687 | 0,350 | 0,000 | 3,855 | 22,430 |
| *1803* | 0,491 | 2,456 | 8,546 | 4,420 | 4,322 | 0,098 | 0,098 | 2,456 | 22,888 |
| *1799* | 0,688 | 2,582 | 10,327 | 2,926 | 3,787 | 0,000 | 0,172 | 2,754 | 23,236 |
| *1795* | 0,338 | 2,142 | 10,598 | 4,171 | 4,735 | 0,338 | 0,113 | 3,269 | 25,705 |
| *1791* | 0,220 | 3,410 | 10,671 | 4,290 | 3,630 | 0,110 | 0,000 | 4,180 | 26,513 |
| *1786* | 0,552 | 1,989 | 12,155 | 4,972 | 2,431 | 0,221 | 0,221 | 3,646 | 26,188 |
| *1782* | 0,214 | 3,632 | 14,423 | 2,350 | 2,671 | 0,107 | 0,534 | 4,060 | 27,991 |
| *1778* | 0,152 | 2,744 | 15,396 | 5,945 | 2,591 | 0,000 | 0,000 | 3,811 | 30,640 |
| *1774* | 0,204 | 2,653 | 10,102 | 2,959 | 1,633 | 0,204 | 0,408 | 4,592 | 22,755 |
| *1770* | 0,214 | 3,529 | 12,941 | 2,888 | 2,888 | 0,214 | 0,214 | 4,064 | 26,952 |
| *1765* | 0,096 | 2,972 | 12,464 | 3,068 | 3,260 | 0,096 | 0,288 | 4,506 | 26,750 |
| *1761* | 0,323 | 2,802 | 13,578 | 3,879 | 2,371 | 0,108 | 0,216 | 5,280 | 28,556 |
| *1757* | 0,078 | 3,333 | 10,775 | 4,419 | 3,023 | 0,233 | 0,155 | 3,488 | 25,504 |
| *1753* | 1,264 | 1,826 | 17,275 | 5,197 | 3,792 | 0,281 | 0,000 | 6,180 | 35,815 |
| *1749* | 0,316 | 2,107 | 8,851 | 3,793 | 2,107 | 0,316 | 0,211 | 5,163 | 22,866 |
| *1744* | 0,377 | 1,759 | 8,920 | 4,271 | 4,146 | 0,126 | 0,503 | 4,020 | 24,121 |
| *1740* | 0,099 | 1,482 | 10,277 | 4,842 | 2,668 | 0,099 | 0,198 | 4,842 | 24,506 |
| *1736* | 0,225 | 2,587 | 8,661 | 3,487 | 2,587 | 0,337 | 0,225 | 3,262 | 21,372 |
| *1732* | 0,426 | 2,215 | 11,073 | 4,344 | 2,215 | 0,341 | 0,170 | 3,066 | 23,850 |
| *1728* | 0,227 | 1,362 | 9,875 | 4,086 | 3,405 | 0,114 | 0,114 | 2,951 | 22,134 |
| *1723* | 0,084 | 3,038 | 8,270 | 3,038 | 2,700 | 0,084 | 0,422 | 2,278 | 19,916 |
| *1719* | 0,697 | 1,742 | 10,366 | 3,484 | 2,700 | 0,348 | 0,000 | 3,049 | 22,387 |
| *1715* | 0,458 | 1,527 | 7,786 | 2,901 | 2,137 | 0,305 | 0,000 | 2,290 | 17,405 |
| *1711* | 0,353 | 1,058 | 9,048 | 2,820 | 3,525 | 0,235 | 0,000 | 2,820 | 19,859 |
| *1707* | 0,255 | 1,851 | 8,424 | 2,616 | 2,234 | 0,128 | 0,128 | 3,318 | 18,953 |
| *1702* | 0,149 | 1,339 | 5,357 | 2,530 | 1,637 | 0,149 | 0,000 | 1,786 | 12,946 |
| *1698* | 0,229 | 2,365 | 8,009 | 3,051 | 2,517 | 0,000 | 0,076 | 3,280 | 19,527 |
| *1694* | 0,000 | 2,699 | 5,997 | 3,148 | 1,949 | 0,300 | 0,150 | 1,949 | 16,192 |
| *1690* | 0,076 | 2,200 | 8,042 | 3,414 | 2,883 | 0,152 | 0,152 | 2,049 | 18,968 |
| *1686* | 0,110 | 2,652 | 12,597 | 2,541 | 2,652 | 0,552 | 0,221 | 5,304 | 26,630 |
| *1681* | 0,407 | 1,424 | 8,037 | 2,747 | 2,340 | 0,102 | 0,102 | 3,052 | 18,210 |
| *1677* | 0,000 | 1,676 | 10,615 | 3,911 | 3,724 | 0,000 | 1,117 | 2,980 | 24,022 |
| *1673* | 0,000 | 1,484 | 8,905 | 3,896 | 2,041 | 0,186 | 0,557 | 2,690 | 19,759 |
| *1669* | 0,061 | 1,284 | 8,496 | 5,257 | 3,423 | 0,550 | 0,244 | 3,117 | 22,433 |
| *1665* | 0,518 | 2,591 | 7,254 | 4,145 | 3,109 | 0,259 | 0,259 | 2,073 | 20,207 |
| *1660* | 0,528 | 1,761 | 7,923 | 4,225 | 4,577 | 0,176 | 0,176 | 4,225 | 23,592 |
| *1656* | 0,219 | 2,407 | 5,689 | 3,720 | 1,313 | 0,000 | 0,000 | 2,845 | 16,193 |
| *1652* | 0,199 | 3,181 | 8,549 | 3,181 | 1,789 | 0,398 | 0,000 | 2,783 | 20,080 |

**Table 10**. Core 1 species absolute abundance and total absolute abundance per sample.

| Year | G. ruber ss | G. ruber sl | G. bulloides | G. inflata | G. truncatulinoides | O. universa | G. ruber pink | Others |
|---|---|---|---|---|---|---|---|---|
| *2013* | 3,109 | 0,518 | 35,233 | 23,834 | 28,497 | 0,000 | 0,000 | 8,808 |
| *2009* | 1,818 | 1,818 | 30,909 | 24,545 | 27,273 | 3,636 | 1,818 | 8,182 |
| *2005* | 1,754 | 2,924 | 45,614 | 16,374 | 22,222 | 1,754 | 1,754 | 7,602 |
| *2000* | 0,699 | 4,196 | 39,860 | 18,182 | 26,573 | 1,399 | 1,399 | 7,692 |
| *1996* | 1,205 | 5,422 | 43,976 | 23,494 | 19,277 | 2,410 | 0,000 | 4,217 |
| *1992* | 1,149 | 3,448 | 33,333 | 28,736 | 20,690 | 3,448 | 0,000 | 9,195 |
| *1988* | 1,681 | 2,521 | 35,294 | 31,933 | 15,966 | 0,000 | 2,521 | 10,084 |
| *1984* | 0,962 | 2,885 | 39,423 | 27,885 | 18,269 | 2,885 | 0,000 | 7,692 |
| *1979* | 3,150 | 0,787 | 45,669 | 24,409 | 14,173 | 1,575 | 0,787 | 9,449 |
| *1975* | 0,000 | 0,913 | 41,096 | 26,484 | 21,005 | 1,370 | 0,457 | 8,676 |
| *1971* | 0,535 | 1,604 | 39,037 | 28,342 | 22,995 | 0,000 | 0,000 | 7,487 |
| *1967* | 0,909 | 2,727 | 41,364 | 19,091 | 23,636 | 3,636 | 0,909 | 7,727 |
| *1963* | 0,685 | 4,795 | 36,301 | 21,233 | 26,712 | 0,000 | 0,685 | 9,589 |
| *1958* | 0,418 | 2,929 | 50,209 | 13,808 | 21,757 | 1,255 | 0,000 | 9,623 |
| *1954* | 0,286 | 2,000 | 47,714 | 21,714 | 18,857 | 2,286 | 0,000 | 7,143 |
| *1950* | 0,873 | 3,057 | 55,895 | 17,031 | 14,410 | 0,873 | 0,000 | 7,860 |
| *1946* | 0,431 | 1,724 | 59,483 | 6,466 | 22,845 | 0,431 | 0,431 | 8,190 |
| *1942* | 1,119 | 4,478 | 49,254 | 14,179 | 20,149 | 0,000 | 1,866 | 8,955 |
| *1937* | 0,365 | 2,920 | 47,445 | 16,058 | 22,628 | 0,730 | 1,095 | 8,759 |
| *1933* | 1,205 | 6,024 | 45,783 | 15,060 | 22,289 | 1,205 | 0,000 | 8,434 |
| *1929* | 0,472 | 2,830 | 49,528 | 21,698 | 14,623 | 0,472 | 1,887 | 8,491 |
| *1925* | 1,434 | 3,943 | 45,161 | 18,280 | 17,563 | 2,509 | 2,151 | 8,961 |
| *1921* | 0,546 | 3,825 | 46,175 | 14,208 | 24,317 | 0,820 | 0,546 | 9,563 |
| *1916* | 1,807 | 4,217 | 57,831 | 11,446 | 13,855 | 1,205 | 0,602 | 9,036 |
| *1912* | 0,444 | 5,778 | 51,111 | 12,889 | 19,111 | 0,889 | 0,444 | 9,333 |
| *1908* | 2,448 | 0,350 | 51,748 | 15,734 | 18,881 | 1,049 | 0,350 | 9,441 |
| *1904* | 0,000 | 2,555 | 44,161 | 24,818 | 18,248 | 1,095 | 0,730 | 8,394 |
| *1900* | 0,746 | 3,483 | 53,234 | 16,667 | 15,423 | 0,746 | 0,249 | 9,453 |
| *1895* | 0,505 | 4,040 | 43,939 | 21,212 | 19,192 | 0,505 | 1,010 | 9,596 |
| *1891* | 0,873 | 3,057 | 45,415 | 24,017 | 16,594 | 0,437 | 0,000 | 9,607 |
| *1887* | 0,935 | 3,271 | 47,196 | 18,224 | 20,093 | 0,467 | 0,467 | 9,346 |
| *1883* | 1,604 | 2,139 | 43,850 | 20,321 | 22,995 | 0,535 | 0,000 | 8,556 |
| *1879* | 1,639 | 3,689 | 38,525 | 25,410 | 18,852 | 0,820 | 1,230 | 9,836 |
| *1874* | 1,558 | 3,636 | 38,961 | 20,779 | 24,935 | 0,779 | 0,000 | 9,351 |
| *1870* | 1,173 | 2,346 | 39,296 | 23,460 | 23,754 | 0,587 | 0,587 | 8,798 |
| *1866* | 1,509 | 6,415 | 47,547 | 21,509 | 12,075 | 1,132 | 0,377 | 9,434 |
| *1862* | 0,958 | 3,834 | 44,089 | 23,003 | 17,252 | 1,278 | 0,319 | 9,265 |
| *1855* | 1,345 | 3,587 | 36,323 | 30,942 | 18,386 | 0,448 | 0,448 | 8,520 |
| *1853* | 0,969 | 2,906 | 43,826 | 20,823 | 21,065 | 1,211 | 0,484 | 8,717 |
| *1849* | 0,595 | 2,381 | 42,857 | 22,619 | 20,833 | 0,000 | 0,595 | 10,119 |
| *1845* | 9,125 | 1,901 | 38,023 | 10,646 | 25,095 | 1,141 | 1,141 | 12,928 |
| *1841* | 2,793 | 11,173 | 34,078 | 23,464 | 20,112 | 0,559 | 0,000 | 7,821 |
| *1837* | 2,273 | 9,848 | 34,091 | 25,758 | 18,182 | 0,758 | 0,000 | 9,091 |
| *1832* | 1,667 | 5,833 | 38,750 | 20,000 | 18,750 | 0,833 | 0,417 | 13,750 |
| *1828* | 1,829 | 15,854 | 38,415 | 10,976 | 23,780 | 1,220 | 0,000 | 7,927 |
| *1824* | 2,139 | 8,021 | 40,107 | 20,856 | 18,182 | 0,535 | 0,535 | 9,626 |
| *1820* | 3,015 | 10,050 | 40,704 | 17,588 | 14,573 | 1,005 | 0,503 | 12,563 |
| *1816* | 2,721 | 12,925 | 40,816 | 15,646 | 15,646 | 1,361 | 0,000 | 10,884 |
| *1812* | 0,526 | 10,526 | 40,000 | 12,632 | 28,947 | 0,526 | 0,000 | 6,842 |
| *1807* | 2,083 | 11,458 | 38,542 | 11,979 | 17,188 | 1,563 | 0,000 | 17,188 |
| *1803* | 2,146 | 10,730 | 37,339 | 18,884 | 19,313 | 0,429 | 0,429 | 10,730 |
| *1799* | 2,963 | 11,111 | 44,444 | 16,296 | 12,593 | 0,000 | 0,741 | 11,852 |
| *1795* | 1,316 | 8,333 | 41,228 | 18,421 | 16,228 | 1,316 | 0,439 | 12,719 |
| *1791* | 0,830 | 12,863 | 40,249 | 13,693 | 16,183 | 0,415 | 0,000 | 15,768 |
| *1786* | 2,110 | 7,595 | 46,414 | 9,283 | 18,987 | 0,844 | 0,844 | 13,924 |
| *1782* | 0,763 | 12,977 | 51,527 | 9,542 | 8,397 | 0,382 | 1,908 | 14,504 |
| *1778* | 0,498 | 8,955 | 50,249 | 8,458 | 19,403 | 0,000 | 0,000 | 12,438 |
| *1774* | 0,897 | 11,659 | 44,395 | 7,175 | 13,004 | 0,897 | 1,794 | 20,179 |
| *1770* | 0,794 | 13,095 | 48,016 | 10,714 | 10,714 | 0,794 | 0,794 | 15,079 |
| *1765* | 0,358 | 11,111 | 46,595 | 12,186 | 11,470 | 0,358 | 1,075 | 16,846 |

| | | | | | | | | |
|---|---|---|---|---|---|---|---|---|
| *1761* | 1,132 | 9,811 | 47,547 | 8,302 | 13,585 | 0,377 | 0,755 | 18,491 |
| *1757* | 0,304 | 13,070 | 42,249 | 11,854 | 17,325 | 0,912 | 0,608 | 13,678 |
| *1753* | 3,529 | 5,098 | 48,235 | 10,588 | 14,510 | 0,784 | 0,000 | 17,255 |
| *1749* | 1,382 | 9,217 | 38,710 | 9,217 | 16,590 | 1,382 | 0,922 | 22,581 |
| *1744* | 1,563 | 7,292 | 36,979 | 17,188 | 17,708 | 0,521 | 2,083 | 16,667 |
| *1740* | 0,403 | 6,048 | 41,935 | 10,887 | 19,758 | 0,403 | 0,806 | 19,758 |
| *1736* | 1,053 | 12,105 | 40,526 | 12,105 | 16,316 | 1,579 | 1,053 | 15,263 |
| *1732* | 1,786 | 9,286 | 46,429 | 9,286 | 18,214 | 1,429 | 0,714 | 12,857 |
| *1728* | 1,026 | 6,154 | 44,615 | 15,385 | 18,462 | 0,513 | 0,513 | 13,333 |
| *1723* | 0,424 | 15,254 | 41,525 | 13,559 | 15,254 | 0,424 | 2,119 | 11,441 |
| *1719* | 3,113 | 7,782 | 46,304 | 12,062 | 15,564 | 1,556 | 0,000 | 13,619 |
| *1715* | 2,632 | 8,772 | 44,737 | 12,281 | 16,667 | 1,754 | 0,000 | 13,158 |
| *1711* | 1,775 | 5,325 | 45,562 | 17,751 | 14,201 | 1,183 | 0,000 | 14,201 |
| *1707* | 1,347 | 9,764 | 44,444 | 11,785 | 13,805 | 0,673 | 0,673 | 17,508 |
| *1702* | 1,149 | 10,345 | 41,379 | 12,644 | 19,540 | 1,149 | 0,000 | 13,793 |
| *1698* | 1,172 | 12,109 | 41,016 | 12,891 | 15,625 | 0,000 | 0,391 | 16,797 |
| *1694* | 0,000 | 16,667 | 37,037 | 12,037 | 19,444 | 1,852 | 0,926 | 12,037 |
| *1690* | 0,400 | 11,600 | 42,400 | 15,200 | 18,000 | 0,800 | 0,800 | 10,800 |
| *1686* | 0,415 | 9,959 | 47,303 | 9,959 | 9,544 | 2,075 | 0,830 | 19,917 |
| *1681* | 2,235 | 7,821 | 44,134 | 12,849 | 15,084 | 0,559 | 0,559 | 16,760 |
| *1677* | 0,000 | 6,977 | 44,186 | 15,504 | 16,279 | 0,000 | 4,651 | 12,403 |
| *1673* | 0,000 | 7,512 | 45,070 | 10,329 | 19,718 | 0,939 | 2,817 | 13,615 |
| *1669* | 0,272 | 5,722 | 37,875 | 15,259 | 23,433 | 2,452 | 1,090 | 13,896 |
| *1665* | 2,564 | 12,821 | 35,897 | 15,385 | 20,513 | 1,282 | 1,282 | 10,256 |
| *1660* | 2,239 | 7,463 | 33,582 | 19,403 | 17,910 | 0,746 | 0,746 | 17,910 |
| *1656* | 1,351 | 14,865 | 35,135 | 8,108 | 22,973 | 0,000 | 0,000 | 17,568 |
| *1652* | 0,990 | 15,842 | 42,574 | 8,911 | 15,842 | 1,980 | 0,000 | 13,861 |

**Table 11**. Core 1 species relative abundance per sample.

| Age model | *G. ruber* ss | *G. ruber* sl | *G. bulloides* | *G. inflata* | *G. truncatulinoides* |
|---|---|---|---|---|---|
| *2013* | 20,7752154 | 16,156837 | 12,2343387 | 28,1594546 | 23,8001515 |
| *2009* | 21,9490739 | 14,7517677 | | | |
| *2005* | 20,2922477 | 13,3942509 | | | |
| *2000* | 9,67379782 | 16,8834504 | | | |
| *1996* | 14,632048 | 14,0159092 | | | |
| *1992* | 16,5530723 | 11,8764939 | 11,1528674 | 27,9176629 | 29,3181497 |
| *1988* | 14,5520243 | 11,2953698 | | | |
| *1984* | 16,2202373 | 15,3017417 | | | |
| *1979* | 21,7544478 | 11,0726388 | | | |
| *1975* | 0 | 15,44754 | | | |
| *1971* | 18,99251 | 17,7697486 | 12,1952634 | 30,4621357 | 25,6307969 |
| *1967* | 21,3470904 | 19,5568333 | | | |
| *1963* | 18,2881883 | 20,0194459 | | | |
| *1958* | 25,5241446 | 16,5075325 | | | |
| *1954* | 19,7785639 | 16,5574983 | | | |
| *1950* | 21,1080556 | 19,8241173 | 12,8489807 | 28,4789562 | 28,2820684 |
| *1946* | 14,8057652 | 16,1296504 | | | |
| *1942* | 20,8686001 | 17,815797 | | | |
| *1937* | 14,8881105 | 20,2141188 | | | |
| *1933* | 15,0503801 | 17,5547648 | | | |
| *1929* | 21,3116897 | 17,0257956 | 12,9334749 | 24,3478531 | 28,2696297 |
| *1925* | 20,1949045 | 19,6803349 | | | |
| *1921* | 18,5489853 | 17,2959107 | | | |
| *1916* | 20,8337346 | 19,7148355 | | | |
| *1912* | 23,0450584 | 19,2330498 | | | |
| *1908* | 14,982814 | 18,7834726 | 13,8729671 | 28,6010559 | 23,9096054 |
| *1904* | 0 | 16,6796715 | | | |
| *1900* | 18,8062652 | 19,2828161 | | | |
| *1895* | 17,6845579 | 18,1004157 | | | |
| *1891* | 20,2225961 | 20,7302997 | | | |
| *1887* | 16,4162682 | 19,6903078 | 12,160619 | 26,007238 | 22,7574471 |
| *1883* | 19,0641437 | 17,0089124 | | | |
| *1879* | 18,3619356 | 18,5835505 | | | |
| *1874* | 17,6285068 | 19,7317632 | | | |
| *1870* | 23,0744091 | 18,2806565 | | | |
| *1866* | 22,1341637 | 20,2036672 | 12,5326246 | 29,5561376 | 27,147522 |
| *1862* | 15,961877 | 19,2595627 | | | |
| *1855* | 18,4638604 | 19,5407124 | | | |
| *1853* | 16,943462 | 18,9474146 | | | |
| *1849* | 16,8338195 | 16,2096214 | 12,8317147 | 22,6903493 | 21,9996794 |
| *1845* | 18,7642682 | 15,9247703 | 12,1786142 | 26,0423142 | 20,2969273 |
| *1841* | 20,0376968 | 18,2228507 | | | |
| *1837* | 16,8343709 | 18,8107029 | | | |
| *1832* | 16,1641954 | 17,1468346 | | | |
| *1828* | 14,981008 | 18,2538956 | 13,4186543 | 29,0268512 | 25,59052 |
| *1824* | 16,2649345 | 19,0610736 | | | |
| *1820* | 14,202679 | 17,4215859 | | | |
| *1816* | 16,5354822 | 18,3861544 | | | |
| *1812* | 0 | 19,5475974 | 12,434545 | 28,5176832 | 19,6923747 |
| *1807* | 18,0172512 | 19,746118 | | | |
| *1803* | 18,9959676 | 15,2310413 | | | |
| *1799* | 20,5081096 | 17,2956192 | | | |
| *1795* | 17,9430672 | 18,2334847 | 11,8208132 | 27,8805113 | 24,0367482 |
| *1791* | 17,1850495 | 16,4864071 | | | |
| *1786* | 17,5725398 | 17,3105232 | | | |
| *1782* | 17,0973972 | 18,3015921 | | | |
| *1778* | 0 | 18,0341107 | 13,353877 | 30,0867218 | 20,8783398 |
| *1774* | 16,2782257 | 17,9609176 | | | |
| *1770* | 15,6494602 | 16,92753 | | | |
| *1765* | 0 | 18,2070321 | | | |
| *1761* | 21,3094553 | 17,089501 | | | |
| *1757* | 0 | 18,4034575 | 13,5196893 | 29,3688271 | 24,8480623 |
| *1753* | 18,0236162 | 16,9755394 | | | |
| *1749* | 17,8084398 | 18,822426 | | | |
| *1744* | 18,2581216 | 18,7589067 | | | |

| | | | | | |
|---|---|---|---|---|---|
| *1740* | 0 | 18,8926581 | | | |
| *1736* | 23,3803442 | 18,0266511 | 11,6152668 | 27,8264038 | 27,8255223 |
| *1732* | 20,6169476 | 19,4956412 | | | |
| *1728* | 17,0217581 | 16,8091551 | | | |
| *1723* | 0 | 18,7280817 | | | |
| *1719* | 19,48007 | 17,6886807 | | | |
| *1715* | 14,0873326 | 18,6334724 | 12,7991033 | 27,5963639 | 22,2958815 |
| *1711* | 15,8404621 | 18,2992354 | | | |
| *1707* | 18,3169147 | 17,9459854 | | | |
| *1702* | 0 | 19,471227 | | | |
| *1698* | 16,8111747 | 20,6012686 | | | |
| *1694* | 0 | 19,1424139 | 10,8449999 | 27,0834677 | 19,8588521 |
| *1690* | 0 | 20,8140009 | | | |
| *1686* | 0 | 17,792893 | | | |
| *1681* | 23,8123644 | 20,0014537 | | | |
| *1677* | 0 | 19,826847 | | | |
| *1673* | 0 | 18,2101935 | 12,6526777 | 27,4426126 | 20,8524808 |
| *1669* | 19,6791618 | 20,3751647 | | | |
| *1665* | 0 | 19,9543321 | | | |
| *1660* | 16,8652756 | 19,5451334 | | | |
| *1656* | 0 | 18,6408889 | | | |
| *1652* | 0 | 17,5066528 | 12,1146566 | 27,0194706 | 22,6692096 |

**Table 12**. Core 1 species Size-Normalized weight (SNW) per sample.